Endocranial shape asymmetries in *Hylobates lar*

By

Soumik Saha

Thesis Advisors:

Dr. Zachary Cofran and Dr. Louis Phillipe Römer

A senior thesis submitted to the Department of Anthropology at Vassar College for the partial fulfillment of the requirements for the degree of Bachelors of Arts with Honors in Anthropology

Vassar College

Poughkeepsie, New York

December 2022

Table of Contents

Abstract

Asymmetries in brain shape, or petalias, is the extension of one cerebral hemisphere beyond the other. In humans, anatomical asymmetry of the brain has been linked to handedness and cognitive functions. Previous research has demonstrated brain shape asymmetries in hominids with a pattern of fluctuating asymmetry. However, non-human great apes show lower variation and a lower degree of fluctuating asymmetry compared to modern humans. This study describes and quantifies the positions of the frontal and occipital petalias of a sample of *Hylobates lar* using 3d models of the cranium and endocranial cavity. Cranial landmarks were used to create a reference system onto which endocast landmarks were projected and the difference between the right and left projections produced the petalial components. This study shows the existence of frontal and occipital petalia in gibbons, and comparison to published literature on the brain shape asymmetry in hominids shows that gibbons have an antisymmetric endocast shape as opposed to the fluctuating asymmetry in hominids. This study also shows that the Broca's area homologue in gibbons does not have the same right asymmetry that is observed in humans and to a lesser extent non-human great apes. This has evolutionary implications indicating that the Yakovlevian anticlockwise torque is unique to great apes, and that the gibbons do not have the same language area functions as humans and other great apes do.

Introduction

Asymmetry in the structure and function of the brain has been observed in both animals and humans. In fact, most biological systems have some level of asymmetry. This is caused by normal variation and specialization of systems (Baianu 2012). In humans and many animals, the two hemispheres of the brain are different anatomically as well as in their function. A careful inspection of the brain reveals asymmetric features between the two hemispheres. This lateralized specialization is thought to be a result of evolutionary and developmental factors (Molfese and Segalowits 1988).

Asymmetries in brain shape, or petalias, is the extension of one cerebral hemisphere beyond the other. In humans, characteristic petalia pattern involves right frontal and left occipital protrusions. The right hemisphere protrudes anteriorly beyond the left (right frontal petalia) and the left hemisphere extends posteriorly beyond the right (left occipital petalia). Along with the petalia, the left occipital lobe often extends across the midline, causing the longitudinal interhemispheric fissure to bend towards the right. This double asymmetry produces the appearance of an anticlockwise twist, hence it is referred to as Yakovlevian anticlockwise torque (LeMay 1976). This specific pattern of lobar asymmetry is typical of the hominin lineage, which includes humans and their ancestors after the evolutionary split from the last common with chimpanzees and bonobos (Holloway 1981; Holloway and de la Costela-Reymondie 1982). It has been observed to be more common in right-handed individuals (LeMay 1976; Kertesz et al. 1986).

One of the earliest discoveries of brain asymmetry was regarding language functions of the brain (Broca 1861; Wernicke 1874). In humans, language functions are specialized in the left hemisphere, resulting in marked volume asymmetry in the Broca's area and Wernicke's area. In patients impacted by strokes or tumors in the left hemisphere, language abilities were found to be more severely impaired compared to those with ailments in the right hemisphere. Language processing and production is localized to the anterior left hemisphere in the pars triangularis (Brodmann area (BA) 44) and pars opercularis (BA 45) of the inferior frontal girus – this area is called the Broca's area. Wernicke's area, on the other hand, is specialized in language comprehension and is associated with BA 21 and 22 in the posterior temporal-parietal region (Cantalupo and Hopkins 2001).

Damage to either language areas results in aphasia, but of different kinds. An injury to the Broca's area results in expressive or non-fluent aphasia. This is characterized by difficulty in speaking fluently, but the comprehension of speech is relatively preserved. Individuals with Broca's aphasia have difficulty in producing grammatically correct sentences and understanding complex grammatical structures, but can still communicate through short utterances ("Broca's (Expressive) Aphasia." 2022). An injury to Wernicke's area causes receptive or fluent aphasia. The ease of producing connected speech is not very affected, but the ability to grasp the meaning of spoken words and sentences is highly impaired. As a result, individuals with Wernicke's aphasia can produce grammatically correct sentences but often without much meaning. This also applies to writing, and individuals usually are not aware that they may be using the wrong or non-existent words ("Wernicke's (Receptive) Aphasia." 2022).

Language areas are also evident in non-human great apes. According to Cantalupo and Hopkins (2001), the three great ape species *Pan troglodytes*, *Pan paniscus* and *Gorilla gorilla* have a homologue of Brodmann's area 44 and in the inferior frontal gyrus, and also have cytoarchitectural and neuroanatomical asymmetries in the substrates showing left hemisphere dominance. In gibbons, the Broca's area homologue has been identified (Shenker 2007), but there has not been neuroanatomical research on the asymmetry in their Broca's area (Figure 1). As such, there is space for further investigation into the Broca's area of gibbons.

This study focuses on observing any asymmetries produced in the region that has been identified as the Broca's area homologue in gibbons. The study of Broca's area in gibbons is particularly interesting, since they have an extraordinarily high diversity in distinctive loud calls which is not common among primates (Geissmann and Orgeldinger 2000). Gibbon vocalizations, or 'songs' are species and sex specific, and have sequential organized structures. Such complex vocal communications are not found in any other apes except humans (Koda 2016). Therefore, gibbons are an excellent species for studies on Broca's area outside of the great apes.

Outside of the Broca's area, there has also been significant research on the asymmetry of the brains of non-human primates. LeMay, Billig, and Geschwind (1982) reported that the different great ape species' endocasts showed asymmetry resembling those of humans; Cercopithecoids (also known as Old World monkeys) showed asymmetry in occipital protrusion on the left side; and Platyrrhines (also known as New World monkeys) showed no significant asymmetry in protrusions. In a small sample of 9 chimpanzees (*Pan troglodytes*), right frontal and left occipital asymmetry was found by Hopkins and Marino (2000), but they detected no asymmetry in cerebral width of Cercopithecoids. On the other hand, Zilles et al. (1996) reported no statistically significant shape asymmetry from a similar sized sample of chimpanzee brains. In a sample of capuchin monkeys (*Cebus apella*), which is a type of Platyrrhine, Phillips and Sherwood (2007) found statistically significant left frontal asymmetry, which is the opposite of that observed in great apes and humans. Falk et al. (1990) reported statistically significant left frontal asymmetry in a large sample of rhesus macaques (*Macaca mulatta*), which is a

Cercopithecoid. More recent research on great apes has revealed that there is a shared pattern of endocranial asymmetry among great apes, modern humans, and fossil hominins (Balzeau, Gilissen, and Grimaud-Hervé 2012). However, the pattern was also found to be more variable in humans than in great apes (Neubauer et al. 2020). Overall, there is a pattern of anterior right hemisphere and posterior left hemisphere asymmetry in humans. This has also been observed in other great apes, but to a lesser variability. In other primates, there has been research showing a variety of asymmetry, but there is no consensus on the patterns of asymmetry outside of the great apes.

One confounding factor of the earlier studies on endocranial asymmetries measured the asymmetries using a variety of methods including observation of brain samples (Holloway and de la Costela-Reymondie 1982), to brain mapping techniques based on computed tomography (CT) and magnetic resonance imaginge (MRI) scanning (LeMay and Kido 1978; Toga and Thompson 2003). Furthermore, studies quantifying petalial asymmetries often used the midsagittal plane of the brain as a geometric midline. However, the existence of a left occipital asymmetry may distort the actual fissure delineating the two hemispheres. Petalial protrusions may make it difficult to identify the midline of the brain and introduce errors to the study. Hopkins and Marino (2000) defined the midline of the brain using landmarks at the interhemispheric fissure at the frontal and occipital poles, and then joining the landmarks with a straight line. This method was further detailed by Balzeau and Gilissen (2010) by using landmarks not only on the endocranial surface, but also on anatomical points of the cranium itself. The most protruding points on the right and left frontal and occipital lobes were projected onto the midplane of the brain as determined by cranial landmarks, and their differences were defined as petalias. Neubauer et al. (2020) on the other hand, used geometric morphometrics and multivariate statistics to avoid specifying the anatomical midplane of the brain. In light of these methodological differences, the present study adopts the methodology detailed by Balzeau and Gilissen (2010) and uses landmarks on both the cranial and endocranial surface. This will provide a reference onto which the endocranial landmarks can be projected and different components of petalia can be measured. As such the results are comparable to previous work on great apes (Balzeau and Gilissen 2010) and humans and fossil hominins (Balzeau, Gilissen, and Grimaud-Hervé 2012).

As detailed above, petalias have been previously studied in many non-human primates, humans, as well as fossil hominins (LeMay 1976; Holloway and de la Costela-Reymondie 1982; LeMay, Billig, and Geschwind 1982; Falk et al. 1990; Balzeau and Gilissen 2010; Balzeau, Gilissen, and Grimaud-Hervé 2012; Balzeau, Ball-Albessard, and Kubicka 2020; Neubauer et al. 2020). However, there is not much research on the brains of gibbons (*Hylobatidae*). Gibbons are the closest evolutionary relatives to hominids, but their endocranial asymmetries are relatively unexplored. Moreover, their calls are highly diverse and distinctive. Commonly referred to as gibbon 'songs', they are analogous to bird sings, in that they are specific to species and to sex. However, the evolution and neuroanatomical backing of gibbon songs is not well understood. Gibbons also co-sing in mother-daughter female specific pairs, and have a specialized form of formant tuning - the only other primate species this is seen in is humans (Koda 2016). Thus, the language areas of gibbon brains are a novel study area that may produce better understanding of the evolution of gibbon songs, and how it compares to the language areas in great apes and humans.

The present confirms the presence of petalias in Lar gibbons (*Hylobates lar*), and quantifies the distribution of the different components of petalia, anteroposterior, vertical, and lateral, in both the frontal and occipital cortex using a sample of 25 Lar gibbon crania in a developmental series from infant to adult. It thus investigates the relationships between these antero-posterior protrusions and the spatial location of the frontal and occipital poles on the two lateral and vertical axes. To further explore the asymmetry in language areas of gibbon brains, this study pursues an observatory analysis of the Broca's area homologue of the gibbon brain. Since gibbons are the closest relatives to great apes, this provides to opportunity to test whether language areas of brain are an ancient cytoarchitectural brain structure that are ancestral to both gibbons and great apes, or if it evolved in the great apes clade and then was further derived in the hominin clade.

Material and methods

The sample used in this study consists of a total of 25 crania of Lar gibbons from the Museum of Comparative Zoology at Harvard University (MCZ). The specimens were collected during the 1937 Asiatic Primate Expedition to present day northern Thailand, specifically from Inthanon Doi (Mount Angka) in Chiang Mai province. The specimens are all wild individuals and are of a variety of ages ranging from infant to adult. The sex of each specimen is known: there are 13 males and 12 females in the sample. Computed tomography (CT) scans of the specimen were generated and then used to produce virtual endocasts of the specimens using a combination of two- and three-dimensional semi-automated segmentation in Avizo software, based on procedures described by Neubauer, Gunz, and Hublin (2009).

First, the cranial bone was defined as a material by setting a gray value range. The foramen magnum was sealed through manual segmentation. At this point, any noticeable artifacts from the CT scan were minimized and any damage to the crania from the capture of the specimens was corrected. Then the three-dimensional segmented bone area was artificially expanded by adding a selected number of voxel layers on the cranial surface. This number varied based on the requirements of the specific specimen, until a cranium with thickened bone but closed small foramina and sutures was produced. This delimited the endocranial cavity completely, and an endocast was produced from it. The endocast was allowed to grow in three dimensions to the same number of voxel layers as the cranial bone altered earlier, so that the endocranial surface matches with the inner surface of the unmodified crania. Finally, further manual corrections were done to rectify any non-exact matches to the inner surface of the cranium.

In order to compare the two hemispheres of the endocast and ascertain asymmetries, landmarks were placed on the endocast and cranium following Balzeau and Gilissen (2010). The cranial landmarks were used as a reference system not influenced by the endocranial cavity shape. While the midsagittal plane can be used as the reference to which the endocast landmarks are projected, this would not account for irregularities in the interhemispheric fissure that separates the two hemispheres. Petalial protrusions may cause the interhemispheric fissure to not follow a medial straight line on the endocranial surface. In humans for example, the left occipital lobe often extends across the midline, causing the interhemispheric fissure to bend towards the right (Holloway 1981). Brain torque influences the midsagittal plane, so if the medial plane of the endocast were to be used to quantify petalia, it would influence the data. So, cranial landmarks were used instead to define an external reference system.

The endocasts produced from CT scans were aligned with the cranium in Avizo, and 7 landmarks were registered (figure 2). On the cranium, the glabella, inion, and basion of each specimen was registered. The glabella is the most anterior midline point on the frontal bone, between the brow ridges or supraorbital tori. The inion is the projecting part of the occipital bone at the midline of the uppermost extensions of the superior nuchal lines. This was not particularly visible in some of the younger specimens, so an approximation of the most posterior point of the occipital bone was used in unclear specimens. The basion is the midpoint of the anterior border of the foramen magnum. These three landmarks formed the basis for the reference system onto which the petalial landmarks were projected. Landmarks were then placed on the most protruding points on the right and left frontal lobes, and the right and left occipital lobes on the endocast. During placement of these landmarks, the endocast was visualized in different positions. It was viewed in a superior, lateral, and anterior or posterior view to precisely define the most protruding point of each lobe.

To describe the variation in the four cranial landmarks, the different components of their spatial location were considered separately. The antero-posterior component of the petalia was determined by considering which one of the right or left most protruding points on the frontal or occipital lobe is located more anteriorly or posteriorly than the other; the lateral component was determined by which one has a more lateral position; and the vertical component was determined by which one is located superior to the other. The components were measured by projecting the endocast landmarks onto the cranial reference. First, the coordinates of two lines and a plane were calculated using the cranial landmarks. The first line (L1) passes through the glabella (G) and the inion (I); the second line (L2) passes through the basion (B) and is orthogonal to L1; the plane is defined by L1 and L2. The four endocast landmarks were first projected orthogonally onto L1. The difference between the projection of the right and left frontal and occipital points gives the antero-posterior component of the frontal and occipital petalias, respectively. The four endocast landmarks were then orthogonally projected onto L2, and the distances between the projections gave the vertical component of the frontal and occipital petalias. Finally, the endocast landmarks were orthogonally projected onto the plane defined by L1 and L2; the difference between the projections produced the lateral component of the frontal and occipital petalias (Figure 3). The differences were calculated such that a positive value indicated a right asymmetry and a negative value indicated a left asymmetry. Therefore, a positive value indicates that the right point is more anterior, lateral, or superior to the left point. In the case of the occipital petalia, a negative value indicates that the left point is more posterior than the right. The calculations to project the landmarks onto lines and planes were conducted in Microsoft Excel (See supplementary materials 1 and 2).

The usage of cranial and endocast landmarks allowed the quantification of endocranial asymmetries using an unbiased reference system. The sample had a large age range since it is a developmental series from infant to adult. While this study did not explore the ontogeny of asymmetry in gibbons, the age range does need to be accounted for. Therefore, a size-correction index was used to standardize the different components of the petalia. The values for asymmetry (mm) were divided by the cubic root of the endocranial volume ($\sqrt[3]{mm^3}$), and then multiplied by 100 to obtain a normalized value to be used in statistical analyses. The sample was also divided into male, female, and all, to analyze the six measured endocranial asymmetry components in terms of the sex of the specimen.

The recorded data were analyzed using multiple statistical procedures, which were all conducted in Microsoft Excel. To find any statistical outliers a two-tailed Grubbs' statistical test was conducted. The Grubbs' test detects a single outlier in a univariate data set that follows an approximately normal distribution. So if any of the specimen's petalia components are drastically different from the rest, it should be detected by Grubbs' test (Table 1).

The relationship between the petalia magnitude and the endocranial size was investigated using parametric linear regression (Table 2) and non-parametric Spearman coefficient of rank correlation (Table 3). Values for kurtosis and skewness were also calculated using Microsoft

Excel. The kurtosis and skewness were analyzed together to detect asymmetry in the sample (Table 4). Skewness is a measurement of the distortion of symmetrical distribution in a dataset. Kurtosis, on the other hand, is a measure of the tailedness of a distribution - i.e. how often outliers occur in the sample. A standard normal distribution has a kurtosis of 3 and is called mesokurtic. Leptokurtic and platykurtic distributions have positive and negative excess kurtosis, respectively. Therefore, leptokurtic distributions have a relatively high probability of extreme events, whereas the opposite is true for platykurtic distributions. The kurtosis values were compared to separate critical values for platykurtosis and leptokurtosis taken from Palmer and Strobeck (2003, table 5, values for equation 7).

Three different types of asymmetry were tested for: directional asymmetry, absolute asymmetry, and FA4a. Signed or directional asymmetry (DA) was obtained by calculating the difference between the right and left side for each petalia in an individual (R - L). A positive DA value indicates a right petalia while a negative value indicates a left petalia. Absolute asymmetry (FA1) was calculated by taking the absolute value of the difference between the two petalia in an individual (|R - L|). Finally, FA4a was also calculated, using the formula $0.798\sqrt{var(R-L)}$ (Bechshøft et al. 2008). This value estimates the variability of the specific petalial component within a sample (Table 5). In a sample with fluctuating asymmetry, the variation is normally distributed with mean of (R - L) being zero. Antisymmetry can be detected by statistical tests for departures of frequency distributions of (R-L) from normality in the direction of platykurtosis.

In order to observe the Broca's area in the endocasts, the endocast meshes were imported to Artec Studio software. Each mesh was duplicated to produce two copies of the endocast, then the copy was mirrored by transforming it by 180° on the x-axis. The two mirrored endocasts were then aligned, and a distance map with error-margin of 3 mm was produced (Figure 4). The inferior frontal gyrus in the anterior left hemisphere contains the Broca's area in humans. In gibbons Brodmann's areas 44 and 45 have been identified to a similar region (Schenker 2007). The corresponding sections of the endocast distance maps were observed and the measured distance difference between the right and left side of the endocrania were measured using the distance maps. The direction of the asymmetry as well as any outliers were noted.

Results

To minimize measurement error, all the landmarks were placed by the same person, and the calculations were cross-checked with Geomagic software. Specimens that had damaged crania were not included in the sample. To determine whether any individuals show outlier values for their petalia components, a two-tailed Grubbs' test statistic was conducted. The Grubbs' test detects a single outlier in a univariate data set that follows an approximately normal distribution. Based on the two-tailed Grubbs' test on the six asymmetries quantified in this study, none of the specimens meet the statistical criteria for outlier status. This ensured that there were no statistical outliers in the sample that could cause a disproportionate impact on the statistical results, leading to misleading interpretations (Table 1).

Next, the relationship between the different petalial components and endocranial volume was investigated. The size corrected data was divided into male, female, and all, and all six measured components of petalia were analyzed using parametric linear regression(Table 2) and non-parametric Spearman rank correlation (Table 3). Of these, the anterior-posterior occipital component in females was found to be correlated with endocranial volume (significant, $0.05 < p < 0.01$) for the Spearman test. None of the other components showed significant correlation in the Spearman test, or in the regression test. However, a non-significant negative correlation was found between antero-posterior occipital, vertical frontal, vertical occipital, and lateral occipital components of all specimens and endocranial capacity, from parametric linear regression. Similarly, a non-significant negative correlation was found between antero-posterior frontal, antero-posterior occipital, and vertical frontal components of all specimen and endocranial capacity, from non-parametric Spearman test. These suggest that with larger endocranial capacity, the proportional asymmetry of the endocranial surface may decrease. Although, since the results are non-significant ($p > 0.05$), this is only a hypothesis that needs to be further investigated. Nevertheless, the lack of concrete correlation between petalial components and endocranial volume indicates variability in the sample.

The asymmetry in the petalial components was measured by investigating three possible patterns of departure from symmetry in a sample: fluctuating asymmetry (FA), directional asymmetry (DA), and antisymmetry (Table 5). The frontal antero-posterior and frontal vertical petalia components showed a right hemisphere asymmetry, as shown by the positive values for directional asymmetry. The frontal lateral and occipital antero-posterior petalial components showed left hemisphere asymmetry, shown by the negative values for directional asymmetry. The occipital vertical and occipital lateral components show directional asymmetry close to zero. The mean absolute asymmetry of the frontal antero-posterior and frontal vertical petalia components are, however, smaller than that of the other four components. This indicates that while these components showed a right hemisphere asymmetry, the degree of asymmetry was higher in the other components. Also, the occipital vertical and occipital lateral components had comparatively high values for absolute asymmetry, which indicates that while they did not show directional asymmetry, the petalia components were still highly variable. This variation was further shown by the FA4a metric that was calculated. FA4a estimates the variability of the specific petalial component within a sample. This was lower in frontal antero-posterior and occipital antero-posterior components of petalia. This indicates that these components had less variability within the sample.

The frequency distribution of size-corrected asymmetry components are shown as histograms in figure 5. Most of the petalia components showed fairly normal distributions, although the antero-posterior occipital and the vertical frontal components were fairly flat. The frontal antero-posterior, occipital antero-posterior, and occipital lateral components show a negative tail. The kurtosis and skewness values obtained are shown in Table 4. The kurtosis values for each component were negative in the full sample for all petalial components except the frontal lateral component. By comparing the p-values to cutoffs obtained from Palmer and Strobeck (2003, table 5, values for equation 7), it was determined that the only occipital vertical and occipital lateral were statistically significantly platykurtic ($p < 0.05$). While the other petalial components were not statistically significantly platykurtic, they were still negative, which provides evidence for platykurtic distribution of the sample, indicating an antisymmetric variation in the endocranial surface of the sample of gibbons.

The observation of the Broca's area homologue on the mirrored endocranial distance maps produced variable results. There were 12 specimens with negative distance in the Broca's area homologue as determined by the distance map, indicating a more pronounced right anterior hemisphere; 8 specimens had positive distance, indicating more pronounced left anterior hemisphere, and 6 specimens had negligible difference between the two sides with distance values close to zero. The small sample size, difficulty in identifying Brodmann's areas 44 and 45 on gibbons, as well as artifacts caused by mirroring the endocast may have contributed to the inconclusive results.

Discussion

Shape asymmetries of the internal table of the cranial vault can be considered as any other standard cranial parameter used for assessing taxonomic distinctiveness. Importantly, the shape of the endocranial cast is commonly used as a proxy for brain shape, as it is in this study. Compared with qualitative assessments of petalial asymmetries, the quantification used in this study to characterize endocranial petalias makes the study repeatable. It also allows further exploration of the morphometric information contained in the analyzed features. Moreover, the use of an external referential, means that the protocol is not influenced by endocranial asymmetries, as it is the case for most previous studies (Balzeau and Gilissen 2010). As such the results are comparable to previous work on great apes (Balzeau and Gilissen 2010) and humans and fossil hominins (Balzeau, Gilissen, and Grimaud-Hervé 2012). Finally, the analysis of ‘‘petalias’’ is based on their original definition: the protrusions of one hemisphere beyond the other (Hadžiselimović and Čuš 1966). Using this unambiguous definition and consistent designation of the analyzed features, along with protocols aimed at detecting and analyzing the different main asymmetry patterns, this study attempts to determine subtle departures from symmetry in *Hylobates lar*.

The first results from the analysis include the parametric linear regression analysis (Table 2) and the non-parametric Spearman rank correlation analysis (Table 3). Of these, the anterior-posterior occipital component in females was found to be correlated with endocranial volume (significant, $0.05 < p < 0.01$) for the Spearman test. None of the other components showed significant correlation in the Spearman test, or in the regression test. Both the regression and Spearman test analysis showed negative correlation between petalial components and endocranial volume, but it was not statistically significant ($p > 0.05$). This indicates that the size corrected petalial components are negatively correlated to endocranial capacity. This has developmental implications for asymmetry in *Hylobates lar*. As the brain size increases, the relative size of the petalia decreases, therefore, the petalial components may remain relatively the same size while the rest of the brain increases in size. However, without more concrete statistically significant evidence, as well as statistical analysis based on developmental stage, this is only a hypothesis. This question may be an interesting topic in *Hylobates lar* endocranial asymmetry for further research.

Next, it emerges from the analysis conducted in this study that the frontal antero-posterior and frontal vertical petalia components show a right hemisphere asymmetry, the frontal lateral and occipital antero-posterior petalial components showed left hemisphere asymmetry, and the occipital vertical and occipital lateral components show directional asymmetry close to zero (Table 5). This indicates that there is a variety of different asymmetries in the *Hylobates lar* petalial components and there is no perceivable directional pattern in the asymmetry. However, in the case of occipital vertical and occipital lateral components, the mean absolute asymmetry (FA1 index) and the FA4a index was comparatively higher than that for other petalia components. These specific components of petalia therefore had even less variability than the other components. However, this still does not show any directional asymmetry in *Hylobates lar*. The frequency distribution histograms (figure 5) also show the lack of any pattern of direction asymmetry.

The final statistical analysis conducted was the skewness and kurtosis analysis. The kurtosis values for each component were negative in the full sample for all petalial components except the frontal lateral component, and they were statistically significantly platykurtic ($p < 0.05$) for the occipital vertical and occipital lateral components. This provides strong evidence for the platykurtic distribution of the petalial components. Platykurtosis indicates that the distributions have a relatively low probability of extreme outliers, rather their distribution is more centered around zero. Also, platykurtic distribution indicates antisymmetric variation in the sample (Palmer 1994). This is markedly different from the fluctuating asymmetry that was determined in great apes (Balzeau, Gilissen, and Grimaud-Hervé 2012). The difference in asymmetry between gibbon and great ape brains indicates that Yakovlevian anticlockwise torque is unique to great apes. This specific type of asymmetry may have allowed hominin brains to become encephalized and develop language and tool related functions.

Finally, the observation of the Broca's area homologue in *Hylobates lar* through distance maps produced by mirroring endocrania produced showed 12 specimens with larger Broca's area homologue on the right hemisphere, 8 specimens with more pronounced left hemisphere Broca's area homologue, and 6 specimens that showed negligible difference between the two sides. While this sample does show more pronounced cytoarchitecture on the right side Broca's area homologue, the sample size is relatively small and there was no statistically significant difference between the two sides. This therefore indicates that gibbons do not have the same language area functions as humans and other great apes do. This brings forth further questions about gibbon vocalization. Are their vocalizations then simply instinctual and not as neuroanatomically elaborate as they may seem to be? It is also possible that gibbons simply have a different area of the brain that is specialized in producing their unique vocal repertoire. Further research into this topic will improve our understanding of gibbon endocranial asymmetry as well as their distinctive vocalization.

Tables

Table 1. Grubb's statistical analysis of six components of petalia in *Hylobates lar*, showing that there are no statistically significant outliers to the data.

	Antero-posterior frontal	Antero-posterior occipital	Vertical frontal	Vertical occipital	Lateral frontal	Lateral occipital
max of Grubb's value	2.07	2.29	2.44	3.40	2.09	2.54
mean of petalia conponent	0.47	-0.43	0.61	0.11	-0.96	0.09
stdev	0.74	1.12	2.32	4.22	3.29	4.71
G	2.81	2.05	1.05	0.81	0.63	0.54
alpha	0.05	0.05	0.05	0.05	0.05	0.05
size	25	25	25	25	25	25
sig value	0.001	0.001	0.001	0.001	0.001	0.001
df	23	23	23	23	23	23
t-crit	3.48	3.48	3.48	3.48	3.48	3.48
G-crit	2.82	2.82	2.82	2.82	2.82	2.82
significant	no	no	no	no	no	no

Table 2. Regression analysis of size-corrected components of petalia in *Hylobates lar*

	Antero-posterior frontal	Antero-posterior occipital	Vertical frontal	Vertical occipital	Lateral frontal	Lateral occipital
Correlation factor (M)	0.35	0.07	-0.14	-0.14	0.46	-0.18
Correlation factor (F)	0.04	-0.32	-0.29	-0.23	-0.20	-0.17
Correlation factor (All)	0.18	-0.11	-0.19	-0.17	0.13	-0.17
T value (M)	1.25	0.23	-0.46	-0.48	1.74	-0.61
T value (F)	0.13	-1.08	-0.97	-0.75	-0.64	-0.56
T value (All)	0.89	-0.53	-0.92	-0.83	0.65	-0.83
df (M)	11	11	11	11	11	11
df (F)	10	10	10	10	10	10
df (All)	23	23	23	23	23	23
p-value (M)	0.24	0.82	0.66	0.64	0.11	0.55
p-value (F)	0.90	0.30	0.35	0.47	0.54	0.59
p-value (All)	0.38	0.60	0.37	0.42	0.52	0.41

Table 3. Spearman correlation analysis of size-corrected components of petalia in *Hylobates lar*

	Antero-posterior frontal	Antero-posterior occipital	Vertical frontal	Vertical occipital	Lateral frontal	Lateral occipital
Spearman coefficient (F)	-0.34	-0.68	-0.33	-0.28	-0.28	0.11
Spearman coefficient (M)	-0.01	0.32	-0.03	0.35	0.38	0.35
Spearman coefficient (All)	-0.16	-0.19	-0.15	0.09	0.06	0.22
T statistic (F)	1.15	2.97	1.12	0.92	0.93	0.34
T statistic (M)	0.03	1.12	0.08	1.24	1.36	1.26
T statistic (All)	0.77	0.90	0.74	0.44	0.30	1.09
df (F)	10	10	10	10	10	10
df (M)	11	11	11	11	11	11
df (All)	23	23	23	23	23	23
p-value (F)	0.28	0.01	0.29	0.38	0.38	0.74
p-value (M)	0.98	0.28	0.93	0.24	0.20	0.23
p-value (All)	0.45	0.37	0.47	0.66	0.77	0.29

Table 4. Kurtosis and skewness indices of size-corrected components of petalia in *Hylobates lar*

Trait		Sex	N	Kurtosis	Kurtosis p-value	Skewness
Frontal	AP	M	13	-1.20742	ns	-0.4428
		F	12	0.23	ns	0.97
		All	25	-0.08	ns	-0.07
	VERT	M	13	-0.44	ns	0.90
		F	12	-0.61	ns	-1.09
		All	25	-0.28	ns	0.34
	LAT	M	13	0.31	ns	0.49
		F	12	0.78	ns	0.02
		All	25	0.93	ns	0.30
Occipital	AP	M	13	0.51	ns	0.09
		F	12	0.13	ns	-0.56
		All	25	-0.94	ns	-0.22
	VERT	M	13	-1.48	*	1.77
		F	12	-1.50	*	-0.90
		All	25	-1.53	*	1.36
	LAT	M	13	-1.40	*	-0.39
		F	12	-1.54	*	-1.26
		All	25	-1.45	*	-0.52

Table 5. Indices of asymmetry in size-corrected components of petalia in *Hylobates lar*

				DA = (R -L)		FA1 = |R-L|		FA4a = 0.798(var(R-L))^1/2
Trait		Sex	N	Mean	SE	Mean	SE	
Frontal	AP	M	13	0.25	0.11	0.42	0.07	0.07
		F	12	0.21	0.08	0.25	0.06	0.03
		All	25	0.23	0.07	0.34	0.05	0.05
	VERT	M	13	0.20	0.26	0.94	0.15	0.63
		F	12	0.33	0.35	0.76	0.23	0.32
		All	25	0.26	0.22	0.85	0.14	0.46
	LAT	M	13	-0.98	0.48	1.34	0.34	0.83
		F	12	0.00	0.40	1.13	0.30	1.09
		All	25	-0.51	0.32	1.24	0.22	1.02
Occipital	AP	M	13	-0.32	0.14	0.50	0.10	0.12
		F	12	-0.10	0.15	0.34	0.10	0.09
		All	25	-0.21	0.10	0.42	0.07	0.11
	VERT	M	13	0.45	0.44	1.44	0.32	2.09
		F	12	-0.43	0.63	1.08	0.50	0.93
		All	25	0.03	0.39	1.27	0.30	1.55
	LAT	M	13	0.08	0.48	1.92	0.35	2.87
		F	12	-0.01	0.74	1.07	0.49	1.09
		All	25	0.04	0.44	1.52	0.31	1.93

Figures

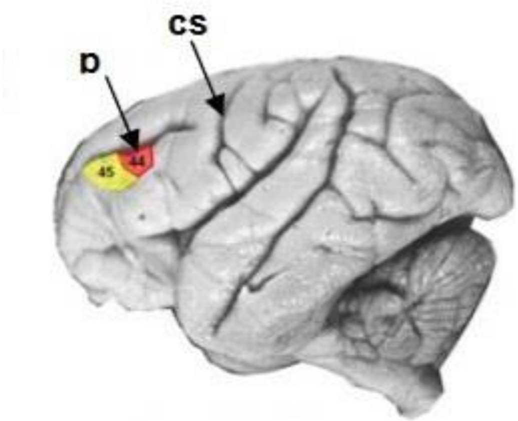

Figure 1. Digital image of the Broca's area homologue in gibbons. Adapted from Schenker (2007).

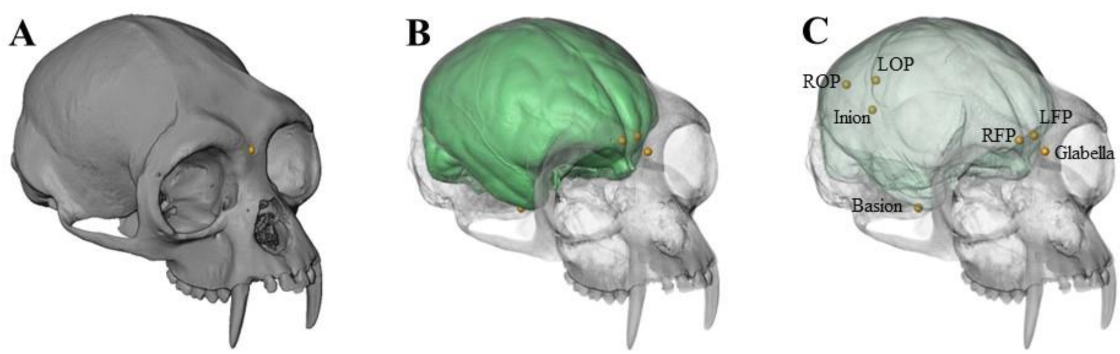

Figure 2. Illustration of the landmarks placed on *Hylobates lar* cranium and endocranium. A: 3D model of *Hylobates lar* cranium. B: Endocast produced from the cranium shown through a semi-transparent cranium. C: Semi-transparent cranium and endocranium showing the positions of the seven landmarks. Three landmarks are positioned on the skull (glabella, basion, inion) and four on the endocranial surface (RFP, LFP: right and left frontal poles, ROP, LOP: right and left occipital poles).

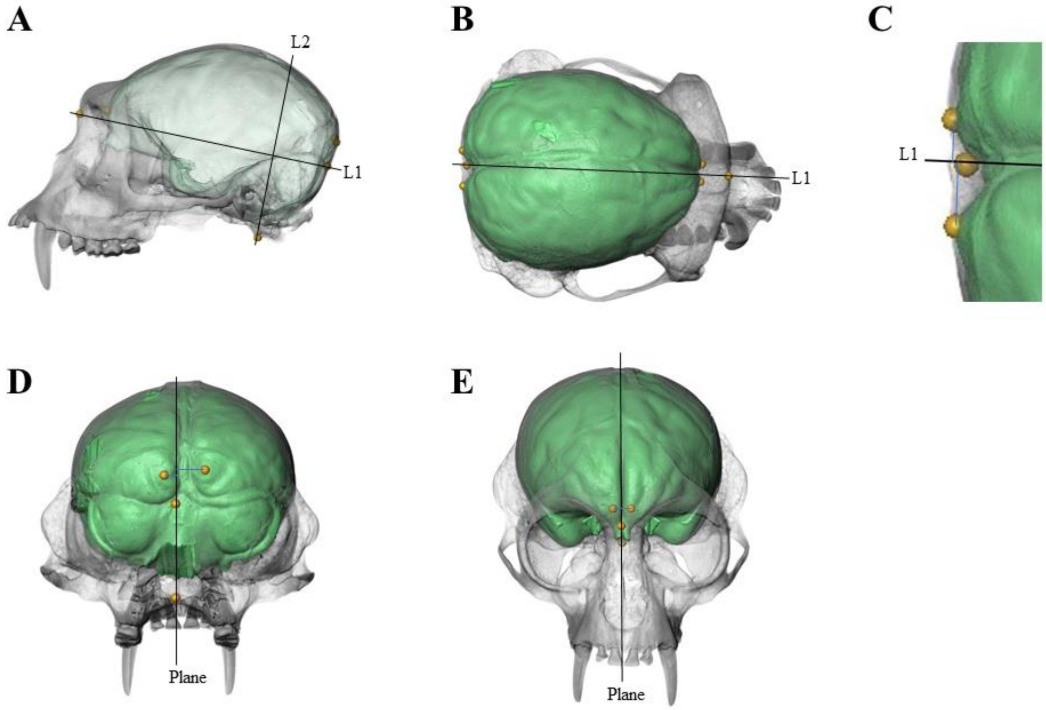

Figure 3. Illustration of the protocol used to quantify the endocranial petalias in *Hylobates lar* endocranium. A: Lateral view showing a line (L1) traced through glabella and inion, and another line (L2) traced through basion orthogonal to L1. B: Superior view showing L1 traced through the glabella and inion. C: Zoomed in superior view showing the orthogonal projection of the right and left occipital poles onto L1. The distance between the projected images of the points corresponds to the occipital antero-posterior component of petalia. D: Posterior view showing a plane that passes through the glabella (not visible), inion, and basion, and the orthogonal distance from the right and left occipital poles to this plane. The difference between the two distances corresponds to the occipital lateral component of petalia. E: Anterior view showing a plane that passes through the glabella, inion (not visible), and basion, and the orthogonal distance from the

right and left frontal poles to this plane. The difference between the two distances corresponds to the frontal lateral component of petalia.

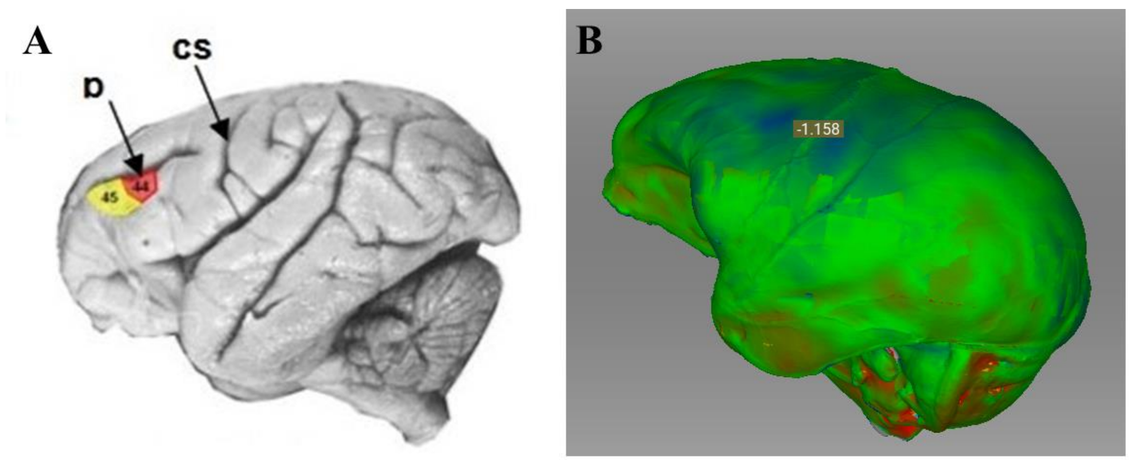

Figure 4. Distance map of *Hylobates lar* brain compared to the Broca’s area homologue in gibbons. A: Digital image of the Broca’s area homologue in gibbons. Adapted from Schenker (2007). B: Distance map of *Hylobates lar* showing blue color and negative in the Broca’s area homologue, indicating that the region is more pronounced on the right hemisphere.

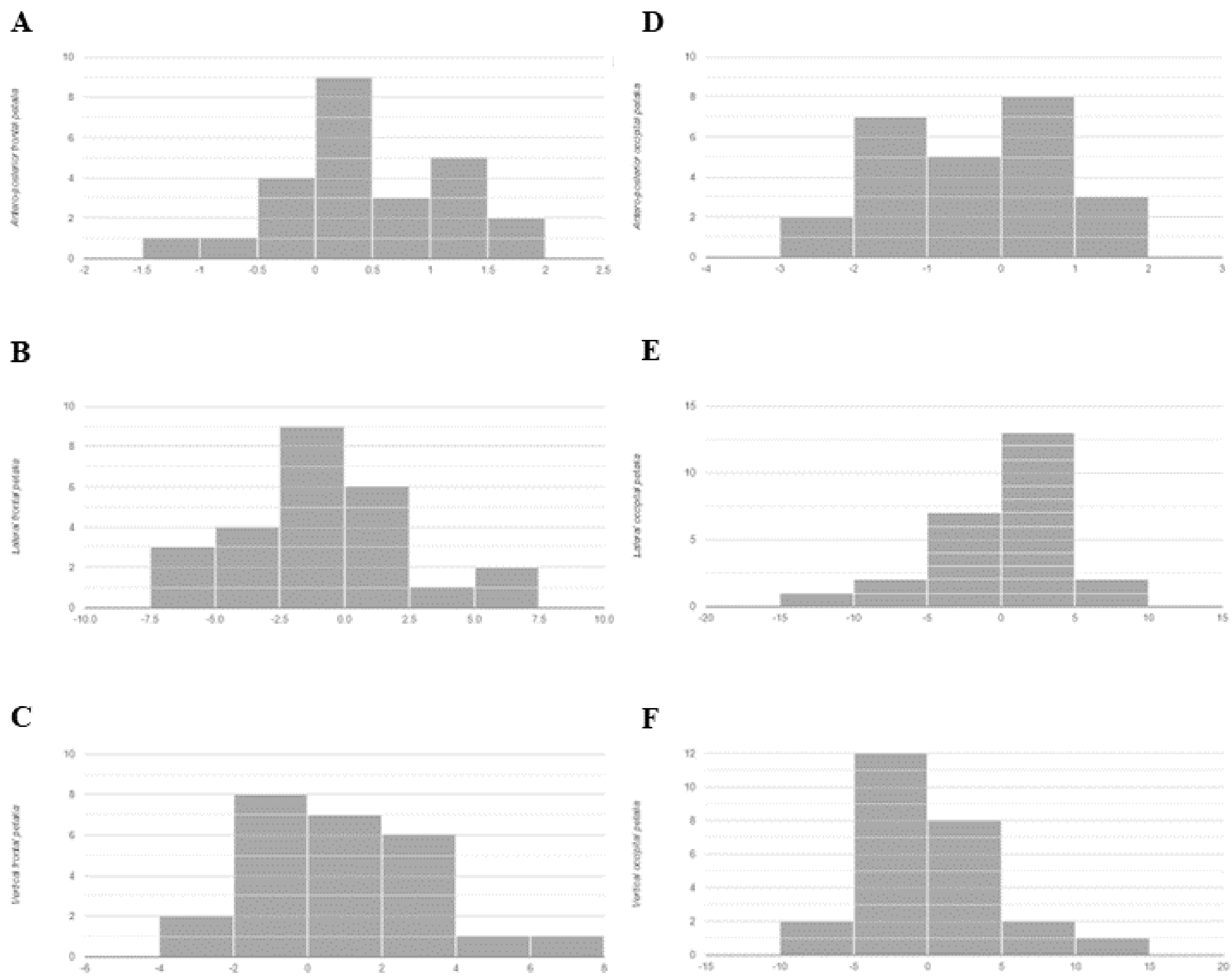

Figure 5. Frequency distribution histograms of petalia components in *Hylobates lar*. The y-axis represents the frequency, while the x-axis represents size-corrected (R-L) petalia. A: Antero-posterior frontal petalia frequency distribution. B: Lateral frontal petalia frequency distribution. C: Vertical frontal petalia frequency distribution. D: Antero-posterior occipital petalia frequency distribution. E: Lateral occipital petalia frequency distribution. F: Vertical occipital petalia frequency distribution.

Supplemental Materials

Supplemental Material 1: Dataset and statistics is a Microsoft Excel sheet that contains the dataset that was obtained from the sample of *Hylobates lar* (n=25), and the statistical analysis that was performed on it. The following table of contents shows the specifics of each sheet in the Excel file. Please see

Sheet number	Title	Contents
2	Data Collection	Landmarks from each individual; calculations done to produce petalial components from landmarks
3	Data Compression	Petalial components; Size correction of petalial components
4	Grubbs test	Size corrected petalial components sorted in ascending order; Grubbs test calculations
5	Spearman Correlation	Spearman correlation calculations
6	Regression	Linear regression calculations
7	Asymmetry	Directional asymmetry, Absolute asymmetry, FA4a, Kurtosis, Skewness

Supplemental Material 2: Calculations is a pdf file containing the vector projection calculation that was done to calculate the components of petalia from the seven landmark coordinates. Please see both supplemental materials attached to this thesis.

Acknowledgements

I would like to thank Professor Zachary Cofran for his imperative assistance in the formation of this thesis. His digitization of Lar gibbon crania from the Museum of Comparative Zoology at Harvard University (MCZ) made this research possible. His help in developing the methodology was indispensable. I would also like to thank Professor Louis Phillipe Römer for his assistance in improving the clarity of the writing.

References

Baianu, I. 2012. "On Asymmetry in Biology and Nature." *Nature Precedings*: 1-1. https://doi.org/10.1038/npre.2012.7134.1.

Balzeau, Antoine, and Emmanuel Gilissen. 2010. "Endocranial Shape Asymmetries in Pan Paniscus, Pan Troglodytes and Gorilla Gorilla Assessed via Skull Based Landmark Analysis." *Journal of Human Evolution* 59 (1): 54–69. https://doi.org/10.1016/j.jhevol.2010.03.013.

Balzeau, Antoine, Emmanuel Gilissen, and Dominique Grimaud-Hervé. 2012. "Shared pattern of endocranial shape asymmetries among great apes, anatomically modern humans, and fossil hominins." *PloS one* 7 (1): e29581. https://doi.org/10.1371/journal.pone.0029581.

Balzeau, Antoine, Lou Ball-Albessard, and Anna Maria Kubicka. 2020. "Variation and correlations in departures from symmetry of brain torque, humeral morphology and handedness in an archaeological sample of Homo sapiens." *Symmetry* 12 (3): 432. https://doi.org/10.3390/sym12030432.

Bechshøft, Thea Ø., Frank F. Rigét, Øystein Wiig, and Christian Sonne. 2008. "Fluctuating asymmetry in metric traits; a practical example of calculating asymmetry, measurement error, and repeatability." *Annales Zoologici Fennici* 45 (1): 32-38. Finnish Zoological and Botanical Publishing Board, 2008.

Broca, Pierre Paul. 1861. "Remarques sur le siège de la faculté du langage articulé, suivies d'une observation d'aphémie (perte de la parole)." *Bulletin de la Société Anthropologique* 6: 330–357.

"Broca's (Expressive) Aphasia." 2022. National Aphasia Association. March 29, 2022. https://www.aphasia.org/aphasia-resources/brocas-aphasia/.

Cantalupo, Claudio, and William D. Hopkins. 2001. "Asymmetric Broca's area in great apes." *Nature* 414: 505-505. https://doi.org/10.1038/35107134.

Geissmann, Thomas, and Mathias Orgeldinger. 2000. "The relationship between duet songs and pair bonds in siamangs, Hylobates syndactylus." *Animal Behaviour* 60 (6): 805-809. https://doi.org/10.1006/anbe.2000.1540.

Hadžiselimović, H., and M. Čuš. 1966. "The appearance of internal structures of the brain in relation to configuration of the human skull." *Cells Tissues Organs* 63 (3): 289-299.

Holloway, Ralph L. 1981. "Volumetric and asymmetry determinations on recent hominid endocasts: Spy I and II, Djebel Ihroud I, and the Salé Homo erectus specimens, with some notes on neandertal brain size." *American Journal of Physical Anthropology* 55 (3): 385-393. https://doi.org/10.1002/ajpa.1330550312.

Holloway, Ralph L., and Marie Christine de la Costela-Reymondie. 1982. "Brain endocast asymmetry in pongids and hominids: some preliminary findings on the paleontology of cerebral dominance." *American Journal of Physical Anthropology* 58 (1): 101-110. https://doi.org/10.1002/ajpa.1330580111.

Hopkins, William D., and Lori Marino. 2000. "Asymmetries in cerebral width in nonhuman primate brains as revealed by magnetic resonance imaging (MRI)." *Neuropsychologia* 38 (4): 493-499.

Kertesz, Andrew, Sandra E. Black, Marsha Polk, and Janice Howell. 1986. “Cerebral Asymmetries on Magnetic Resonance Imaging.” *Cortex* 22 (1): 117–27. https://doi.org/10.1016/S0010-9452(86)80036-3.

Koda, Hiroki. 2016. "Gibbon songs: Understanding the evolution and development of this unique form of vocal communication." In *Evolution of gibbons and siamang* edited by Ulrich H. Reichard, Hirohisa Hirai, and Claudia Barelli, 349-359. Springer, New York. https://doi.org/10.1007/978-1-4939-5614-2_15.

LeMay, Marjorie. 1976. “Morphological Cerebral Asymmetries of Modern Man, Fossil Man, and Nonhuman Primate.” *Annals of the New York Academy of Sciences* 280: 349–66. https://doi.org/10.1111/j.1749-6632.1976.tb25499.x.

LeMay, Marjorie, and Daniel K. Kido. 1978. “Asymmetries of the cerebral hemispheres on computed tomograms.” *Journal of computer assisted tomography* 2 (4): 471–476. https://doi.org/10.1097/00004728-197809000-00018.

LeMay, Marjorie, Michael S. Billig, and Norman Geschwind. 1982. "Asymmetries of the brains and skulls of nonhuman primates." In *Primate brain evolution Methods and Concepts* edited by Este Armstrong and Dean Falk, 263-277. Boston: Springer. https://doi.org/10.1007/978-1-4684-4148-2_17.

Molfese, Dennis L., and Sidney J. Segalowitz. 1988. *Brain Lateralization in children: Developmental implications*. Guilford Press.

Neubauer, Simon, Philipp Gunz, and Jean-Jacques Hublin. 2009. "The pattern of endocranial ontogenetic shape changes in humans." *Journal of anatomy* 215 (3): 240-255. https://doi.org/10.1111/j.1469-7580.2009.01106.x.

Neubauer, Simon, Philipp Gunz, Nadia A. Scott, Jean-Jacques Hublin, and Philipp Mitteroecker. 2020. "Evolution of brain lateralization: A shared hominid pattern of endocranial asymmetry is much more variable in humans than in great apes." *Science advances* 6 (7): eaax9935. https://doi.org/10.1126/sciadv.aax9935.

Palmer, A. Richard. 1994. "Fluctuating asymmetry analyses: a primer." In *Developmental instability: its origins and evolutionary implications* edited by Therese Ann Markow, 335-364. Kluwer Academic Publishers, Dordrecht.

Palmer, A. Richard, and Curtis Strobeck. 2003. "CH 17. Fluctuating asymmetry analyses revisited." In *Developmental Instability: Causes and Consequences* edited by Michal Polak, 279-319. Oxford University Press: Oxford.

Phillips, Kimberley A., and Chet C. Sherwood. 2007. "Cerebral petalias and their relationship to handedness in capuchin monkeys (Cebus apella)." *Neuropsychologia* 45 (10): 2398-2401. https://doi.org/10.1016/j.neuropsychologia.2007.02.021.

Schenker, Natalie Marie. 2007. “Comparative analysis of Broca's area in hominoids.” PhD diss. University of California, San Diego. https://escholarship.org/uc/item/7br1r08t.

Toga, Arthur W., and Paul M. Thompson. 2003. “Mapping Brain Asymmetry.” *Nature Reviews Neuroscience* 4 (1): 37–48. https://doi.org/10.1038/nrn1009.

Wernicke, Carl. 1874. *Der aphasische Symptomencomplex: eine psychologische Studie auf anatomischer Basis*. Cohn und Welgert, Cohn und Welgert, Breslau.

“Wernicke's (Receptive) Aphasia.” 2022. National Aphasia Association. March 29, 2022. https://www.aphasia.org/aphasia-resources/wernickes-aphasia/.

Zilles, Karl, Andreas Dabringhaus, Stefan Geyer, Katrin Amunts, Meishu Qü, Axel Schleicher, Emmanuel Gilissen, Gottfried Schlaug, and Helmut Steinmetz. 1996. "Structural asymmetries in the human forebrain and the forebrain of non-human primates and rats." *Neuroscience & Biobehavioral Reviews* 20 (4): 593-605. https://doi.org/10.1016/0149-7634(95)00072-0.

Supplementary Material 1: Dataset and statistics
Endocranial shape asymmetries in *Hylobates lar*
Soumik Saha

Table of Contents

2. Data Collection: Landmarks from each individual; calculations done to produce petalial components from landmarks

Id number	Age category	Sex	Landmark	x	y	z	Vectors	x	y	z	Scalars		Points	x	y	z	Components of patella (right+)	
41413	Adult	M	Glabella(G)	36.12	33.41112	47.67841	(L1)d=I - G	5.9598	73.93	-30.2	t (RFP)	0.080241	RFP onto L1	36.59822	39.34301	45.25832	Antero-posterior frontal	0.564858
			Inion (I)	42.0798	107.337	17.5182	RFP-G	-0.877	6.81	-0.53	t (LFP)	0.087296	LFP onto L1	36.64027	39.86456	45.04554	Antero-posterior occipital	-0.48562
			Basion (B)	41.1166	78.50108	7.3444	LFP-G	4.2542	6.724	-1.23	t (ROP)	0.98472	ROP onto L1	41.98873	106.2074	17.97906		
			Right Frontal Pole (RFP)	35.24269	40.22145	47.14362	ROP-G	-4.307	75.81	-24.3	t (LOP)	0.990785	LOP onto L1	42.02488	106.6558	17.79613		
			Left Frontal Pole (LFP)	40.37419	40.13503	46.44632	LOP-G	13.987	74.67	-24.8	t (B)	0.714421	B onto L1	40.37781	86.22531	26.13132		
			Right Occipital Pole (ROP)	31.81292	109.2187	23.34929	B-G	4.9966	45.09	-40.3								
			Left Occipital Pole (LOP)	50.10669	108.0771	22.87695												
							(L2)d=B onto L1 - B	-0.739	7.724	18.79	t (RFP)	1.104574	RFP onto L2	40.30055	87.03306	28.09595	Vertical frontal	-0.86384
							RFP-B	-5.874	-38.3	39.8	t (LFP)	1.062076	LFP onto L2	40.33194	86.70479	27.29753	Vertical occipital	-1.53531
							LFP-B	-0.742	-38.4	39.1	t (ROP)	1.318687	ROP onto L2	40.14236	88.68692	32.11847		
							ROP-B	-9.304	30.72	16	t (LOP)	1.243154	LOP onto L2	40.19817	88.10348	30.69943		
							LOP-B	8.9901	29.58	15.53								
							N of Plain	-1622	89.68	-101	RFP to P	1.282674					Lateral frontal	-2.51014
											LFP to P	3.792818					Lateral occipital	1.684713
											ROP to P	9.974655						
											LOP to P	8.289941						
41415	Adult	M	Glabella(G)	40.98746	80.10648	43.79057	(L1)d=I - G	-0.934	-76.4	-16.7	t (RFP)	0.095851	RFP onto L1	40.8979	72.78047	42.19043	Antero-posterior frontal	0.172272
			Inion (I)	40.0531	3.675181	27.09658	RFP-G	3.9181	-8.55	3.768	t (LFP)	0.098053	LFP onto L1	40.89584	72.61218	42.15367	Antero-posterior occipital	-1.39427
			Basion (B)	39.24331	27.65729	7.724082	LFP-G	-3.699	-8.65	3.839	t (ROP)	0.971466	ROP onto L1	40.07976	5.85607	27.57292		
			Right Frontal Pole (RFP)	44.9056	71.55902	47.55836	ROP-G	5.2528	-76.2	-7.8	t (LOP)	0.989287	LOP onto L1	40.06311	4.494015	27.27543		
			Left Frontal Pole (LFP)	37.28817	71.46034	47.62912	LOP-G	-9.793	-77	-9.8	t (B)	0.753513	B onto L1	40.28341	22.51451	31.21143		
			Right Occipital Pole (ROP)	46.24027	3.942779	35.98788	B-G	-1.744	-52.4	-36.1								
			Left Occipital Pole (LOP)	31.19457	3.134765	33.99495												
							(L2)d=B onto L1 - B	1.0401	-5.14	23.49	t (RFP)	1.235725	RFP onto L2	40.52858	21.30223	36.74798	Vertical frontal	-0.23907
							RFP-B	5.6623	43.9	39.83	t (LFP)	1.225791	LFP onto L2	40.51825	21.35332	36.51467	Vertical occipital	-2.42257
							LFP-B	-1.955	43.8	39.91	t (ROP)	1.369298	ROP onto L2	40.66751	20.61529	39.88527		
							ROP-B	6.997	-23.7	28.26	t (LOP)	1.268636	LOP onto L2	40.56281	21.13298	37.52098		
							LOP-B	-8.049	-24.5	26.27								
							N of Plain	1881	-4.58	-84.3	RFP to P	3.766312					Lateral frontal	-0.08008
											LFP to P	3.84639					Lateral occipital	-3.37493
											ROP to P	5.782222						
											LOP to P	9.157156						
41422	Juv1	F	Glabella(G)	42.2244	21.239	43.112	(L1)d=I - G	11.285	67.96	-22.3	t (RFP)	0.017252	RFP onto L1	42.41909	22.41152	42.72809	Antero-posterior frontal	0.091424
			Inion (I)	53.5096	89.2038	20.8586	RFP-G	-1.602	2.125	1.615	t (LFP)	0.018515	LFP onto L1	42.43334	22.49734	42.69999	Antero-posterior occipital	0.056599
			Basion (B)	47.233	59.5326	6.5936	LFP-G	4.2566	1.203	1.471	t (ROP)	1.001668	ROP onto L1	53.52843	89.31719	20.82147		
			Right Frontal Pole (RFP)	40.62262	23.36444	44.72741	ROP-G	7.0558	70.49	-17.1	t (LOP)	1.000887	LOP onto L1	53.5196	89.26406	20.83887		
			Left Frontal Pole (LFP)	46.48101	22.44178	44.58296	LOP-G	16.635	67.36	-21.6	t (B)	0.662332	B onto L1	49.69894	66.25423	28.37287		
			Right Occipital Pole (ROP)	49.28024	91.72563	26.02282	B-G	5.0086	38.29	-36.5								
			Left Occipital Pole (LOP)	58.85965	88.597	21.50965												
							(L2)d=B onto L1 - B	2.4659	6.722	21.78	t (RFP)	1.086604	RFP onto L2	49.9125	66.83635	30.25905	Vertical frontal	0.2224
							RFP-B	-6.61	-36.2	38.13	t (LFP)	1.096305	LFP onto L2	49.93643	66.90156	30.47032	Vertical occipital	-4.17435
							LFP-B	-0.752	-37.1	37.99	t (ROP)	1.226398	ROP onto L2	50.25723	67.77599	33.30366		
							ROP-B	2.0472	32.19	19.43	t (LOP)	1.044318	LOP onto L2	49.80823	66.55212	29.33809		
							LOP-B	11.627	29.06	14.92								
							N of Plain	-1630	300.7	91.74	RFP to P	2.047077					Lateral frontal	-1.83333
											LFP to P	3.880409					Lateral occipital	-0.4321
											ROP to P	4.89506						
											LOP to P	5.327163						
41425	Juv1	F	Glabella(G)	28	75.25001	32.4	(L1)d=I - G	3	-71.5	-11	t (RFP)	0.020096	RFP onto L1	28.06029	73.81412	32.17894	Antero-posterior frontal	0.057194
			Inion (I)	31	3.8	21.4	RFP-G	2.3569	-1.94	3.663	t (LFP)	0.020887	LFP onto L1	28.06266	73.75764	32.17024	Antero-posterior occipital	0.046092
			Basion (B)	30.35	30.65	3.6	LFP-G	-2.341	-2.09	2.986	t (ROP)	1.016433	ROP onto L1	31.0493	2.625887	21.21924		
			Right Frontal Pole (RFP)	30.3569	73.31259	36.06291	ROP-G	7.9455	-74	-0.67	t (LOP)	1.015796	LOP onto L1	31.04739	2.671402	21.22625		
			Left Frontal Pole (LFP)	25.65917	73.16167	35.38583	LOP-G	-1.764	-74.2	-2.08	t (B)	0.670573	B onto L1	30.01172	27.33754	25.02369		
			Right Occipital Pole (ROP)	35.94552	1.213867	31.72629	B-G	2.35	-44.6	-28.8								
			Left Occipital Pole (LOP)	26.23639	1.068665	30.32467												
							(L2)d=B onto L1 - B	-0.338	-3.31	21.42	t (RFP)	1.178899	RFP onto L2	29.9512	26.74494	28.85637	Vertical frontal	-0.57269
							RFP-B	0.0069	42.66	32.46	t (LFP)	1.152484	LFP onto L2	29.96014	26.83244	28.29047	Vertical occipital	-1.21131
							LFP-B	-4.691	42.51	31.79	t (ROP)	1.4853	ROP onto L2	29.84755	25.73	35.4206		
							ROP-B	5.5955	-29.4	28.13	t (LOP)	1.42943	LOP onto L2	29.86645	25.91507	34.22366		
							LOP-B	-4.114	-29.6	26.72								
							N of Plain	1567.2	60.55	34.11	RFP to P	2.359444					Lateral frontal	0.005227
											LFP to P	2.354218					Lateral occipital	0.395046
											ROP to P	5.065363						
											LOP to P	4.670317						
41428	Adult	M	Glabella(G)	41.5415	83.25697	56.0084	(L1)d=I - G	1.2782	-78.6	-0.99	t (RFP)	0.104716	RFP onto L1	41.67535	75.03143	55.90498	Antero-posterior frontal	-0.14011
			Inion (I)	42.8197	4.706081	55.0207	RFP-G	2.7561	-8.21	2.348	t (LFP)	0.102933	LFP onto L1	41.67307	75.1715	55.90674	Antero-posterior occipital	-0.75874
			Basion (B)	40.7281	21.67122	29.1662	LFP-G	-2.485	-8.16	2.759	t (ROP)	1.00494	ROP onto L1	42.82602	4.318002	55.01582		
			Right Frontal Pole (RFP)	44.29755	75.04327	58.3561	ROP-G	9.6713	-78.9	7.777	t (LOP)	1.014598	LOP onto L1	42.83836	3.559421	55.00628		
			Left Frontal Pole (LFP)	39.05601	75.09295	58.7672	LOP-G	-1.399	-79.8	6.863	t (B)	0.787819	B onto L1	42.54849	21.37311	55.23027		
			Right Occipital Pole (ROP)	51.21281	4.3442	63.78574	B-G	-0.813	-61.6	-26.8								
			Left Occipital Pole (LOP)	40.14254	3.416656	62.87149												
							(L2)d=B onto L1 - B	1.8204	-0.3	26.06	t (RFP)	1.10056	RFP onto L2	42.73155	21.34313	57.85128	Vertical frontal	0.044335
							RFP-B	3.5695	53.37	29.19	t (LFP)	1.102257	LFP onto L2	42.73464	21.34262	57.8955	Vertical occipital	-1.67264
							LFP-B	-1.672	53.42	29.6	t (ROP)	1.357149	ROP onto L2	43.19864	21.26664	64.53903		
							ROP-B	10.485	-17.3	34.62	t (LOP)	1.293135	LOP onto L2	43.08211	21.28572	62.87056		
							LOP-B	-0.586	-18.3	33.71								
							N of Plain	2047.7	35.11	-143	RFP to P	2.44541					Lateral frontal	-0.365
											LFP to P	2.810414					Lateral occipital	4.518775
											ROP to P	7.756516						
											LOP to P	3.237741						
41431	Adult	M	Glabella(G)	52.76206	76.09267	50.48263	(L1)d=I - G	0.067	-22.5	-33.7	t (RFP)	0.087072	RFP onto L1	52.76789	74.13712	47.55223	Antero-posterior frontal	0.371725
			Inion (I)	52.82909	53.6336	16.82754	RFP-G	2.9208	-11.2	3.242	t (LFP)	0.096259	LFP onto L1	52.76851	73.93078	47.24303	Antero-posterior occipital	0.781156
			Basion (B)	54.03585	32.85058	50.2815	LFP-G	-4.154	-9.18	1.433	t (ROP)	1.147969	ROP onto L1	52.83901	50.31036	11.84763		
			Right Frontal Pole (RFP)	55.6829	64.8971	53.72418	ROP-G	4.6443	-52.4	-20.9	t (LOP)	1.128662	LOP onto L1	52.83772	50.74396	12.4974		
			Left Frontal Pole (LFP)	48.60776	66.91628	51.91574	LOP-G	-8.063	-46.7	-23.7	t (B)	0.597425	B onto L1	52.80211	62.67507	30.37625		
			Right Occipital Pole (ROP)	57.40632	23.69375	29.6188	B-G	1.2738	-43.2	-0.2								
			Left Occipital Pole (LOP)	44.69949	29.37326	26.7425												
							(L2)d=B onto L1 - B	-1.234	29.82	-19.9	t (RFP)	0.687681	RFP onto L2	53.18743	53.36032	36.59303	Vertical frontal	2.925101
							RFP-B	1.647	32.05	3.443	t (LFP)	0.76921	LFP onto L2	53.08684	55.79188	34.97018	Vertical occipital	6.753946
							LFP-B	-5.428	34.07	1.634	t (ROP)	0.10413	ROP onto L2	53.90738	35.9562	48.20877		
							ROP-B	3.3705	-9.16	-20.7	t (LOP)	0.292377	LOP onto L2	53.67514	41.57056	44.46167		
							LOP-B	-9.336	-3.48	-23.5								
							N of Plain	-1451	-42.9	25.71	RFP to P	2.531183					Lateral frontal	-1.91693
											LFP to P	4.448118					Lateral occipital	-5.55252
											ROP to P	3.464077						
											LOP to P	9.016601						
41437	Juv2	F	Glabella(G)	52.75111	74.33111	46.97169	(L1)d=I - G	-0.123	-67.4	-32.6	t (RFP)	0.039289	RFP onto L1	52.74628	71.6837	45.69147	Antero-posterior frontal	0.290764
			Inion (I)	52.62815	6.947407	14.38662	RFP-G	2.4817	-3.77	1.03	t (LFP)	0.043173	LFP onto L1	52.74581	71.42193	45.56489	Antero-posterior occipital	-0.00175
			Basion (B)	52.62815	34.49111	4.979983	LFP-G	-2.891	-4.15	1.172	t (ROP)	1.007761	ROP onto L1	52.6272	6.424453	14.13373		
			Right Frontal Pole (RFP)	55.23281	70.56201	48.00166	ROP-G	5.8442	-71.3	-25.8	t (LOP)	1.007784	LOP onto L1	52.62719	6.422874	14.13297		
			Left Frontal Pole (LFP)	49.86016	70.18019	48.14362	LOP-G	-5.669	-71.2	-26	t (B)	0.723424	B onto L1	52.66216	25.58413	23.39887		
			Right Occipital Pole (ROP)	58.59532	3.030228	21.13024	B-G	-0.123	-39.8	-42								
			Left Occipital Pole (LOP)	47.08195	3.143684	20.93503												
							(L2)d=B onto L1 - B	0.034	-8.91	18.42	t (RFP)	1.125723	RFP onto L2	52.66644	24.46432	25.71455	Vertical frontal	0.285095
							RFP-B	2.6047	36.07	43.02	t (LFP)	1.139657	LFP onto L2	52.66691	24.34021	25.97121	Vertical occipital	-0.24427
							LFP-B	-2.768	35.69	43.16	t (ROP)	1.38057	ROP onto L2	52.6751	22.19441	30.40855		
							ROP-B	5.9672	-31.5	16.15	t (LOP)	1.368631	LOP onto L2	52.6747	22.30075	30.18865		

							LOP-B	-5.546	-31.3	15.96								
							N of Plain	1531.4	-1.16	-3.39	RFP to P	2.482263					Lateral frontal	-0.40814
											LFP to P	2.890406					Lateral occipital	0.397404
											ROP to P	5.955195						
											LOP to P	5.557791						
41438	Juv2	F	Glabella(G)	46.3182	16.796	36.1114	(L1)d=I - G	0.7106	68.61	-11.5	t (RFP)	0.0248	RFP onto L1	46.33583	18.4974	35.82623	Antero-posterior frontal	0.450898
			Inion (I)	47.0288	85.40121	24.6126	RFP-G	-3.203	2.438	3.909	t (LFP)	0.031281	LFP onto L1	46.34043	18.94207	35.7517	Antero-posterior occipital	0.654649
			Basion (B)	47.4164	60.401	10.013	LFP-G	2.9883	3.08	5.398	t (ROP)	1.033917	ROP onto L1	47.0529	87.72809	24.2226		
			Right Frontal Pole (RFP)	43.11498	19.23377	40.02059	ROP-G	-6.279	72.38	-3.66	t (LOP)	1.024507	LOP onto L1	47.04622	87.08248	24.3308		
			Left Frontal Pole (LFP)	49.30653	19.87642	41.50959	LOP-G	6.9159	72.05	-0.88	t (B)	0.680334	B onto L1	46.80165	63.47047	28.28837		
			Right Occipital Pole (ROP)	40.03917	89.1803	32.45345	B-G	1.0982	43.61	-26.1								
			Left Occipital Pole (LOP)	53.23409	88.84488	35.22817												
							(L2)d=B onto L1 - B	-0.615	3.069	18.28	t (RFP)	1.235301	RFP onto L2	46.657	64.19272	32.58858	Vertical frontal	1.368735
							RFP-B	-4.301	-41.2	30.01	t (LFP)	1.309121	LFP onto L2	46.61161	64.41931	33.93767	Vertical occipital	2.24188
							LFP-B	1.8901	-40.5	31.5	t (ROP)	1.463049	ROP onto L2	46.51699	64.89179	36.75076		
							ROP-B	-7.377	28.78	22.44	t (LOP)	1.58396	LOP onto L2	46.44266	65.26292	38.96046		
							LOP-B	5.8177	28.44	25.22								
							N of Plain	-1289	5.918	-44.4	RFP to P	3.078048					Lateral frontal	-0.07998
											LFP to P	3.158029					Lateral occipital	0.182312
											ROP to P	6.733121						
											LOP to P	6.550809						
41447	Adult	M	Glabella(G)	55.5444	26.7066	28.2384	(L1)d=I - G	0.5328	83.12	-2.8	t (RFP)	0.105521	RFP onto L1	55.60062	35.47715	27.94324	Antero-posterior frontal	0.142936
			Inion (I)	56.0772	109.8234	25.4412	RFP-G	3.4707	8.743	-0.48	t (LFP)	0.107239	LFP onto L1	55.60154	35.62	27.93843	Antero-posterior occipital	0.111461
			Basion (B)	53.946	89.0442	56.1438	LFP-G	-3.317	8.934	-0.33	t (ROP)	0.969489	ROP onto L1	56.06095	107.2875	25.52655		
			Right Frontal Pole (RFP)	59.01508	35.44915	27.76178	ROP-G	7.4886	80.52	-3.05	t (LOP)	0.968149	LOP onto L1	56.06023	107.1761	25.5303		
			Left Frontal Pole (LFP)	52.22714	35.64061	27.90819	LOP-G	-7.547	80.4	-6.42	t (B)	0.737712	B onto L1	55.93745	88.02287	26.17487		
			Right Occipital Pole (ROP)	63.033	107.2314	25.18917	B-G	-1.598	62.34	27.91								
			Left Occipital Pole (LOP)	47.99717	107.103	21.82283												
							(L2)d=B onto L1 - B	1.9915	-1.02	-30	t (RFP)	1.013582	RFP onto L2	55.9645	88.009	25.76784	Vertical frontal	-0.60231
							RFP-B	5.0691	-53.6	-28.4	t (LFP)	0.99354	LFP onto L2	55.92459	88.02947	26.36848	Vertical occipital	2.364995
							LFP-B	-1.719	-53.4	-28.2	t (ROP)	1.026632	ROP onto L2	55.99049	87.99567	25.37675		
							ROP-B	9.087	18.19	-31	t (LOP)	1.105328	LOP onto L2	56.14721	87.91529	23.01832		
							LOP-B	-5.949	18.06	-34.3								
							N of Plain	2493.8	-10.4	166.1	RFP to P	3.394943					Lateral frontal	0.02594
											LFP to P	3.369003					Lateral occipital	-1.35682
											ROP to P	6.9344						
											LOP to P	8.291216						
41461	Juv2	M	Glabella(G)	47.3171	23.79184	39.1867	(L1)d=I - G	5.2649	74.44	-13.6	t (RFP)	0.040419	RFP onto L1	47.5299	26.80071	38.63718	Antero-posterior frontal	0.689388
			Inion (I)	52.58196	98.23297	25.59131	RFP-G	-1.267	3.043	-0.94	t (LFP)	0.049508	LFP onto L1	47.57775	27.47724	38.51362	Antero-posterior occipital	-0.56289
			Basion (B)	54.3147	72.70839	8.197218	LFP-G	4.8027	3.368	-0.65	t (ROP)	0.974307	ROP onto L1	52.44669	96.32037	25.94062		
			Right Frontal Pole (RFP)	46.04989	26.83451	38.2491	ROP-G	-0.659	73.54	-9.94	t (LOP)	0.981728	LOP onto L1	52.48576	96.87276	25.83973		
			Left Frontal Pole (LFP)	52.11977	27.15983	38.53453	LOP-G	10.488	73.54	-8.77	t (B)	0.712467	B onto L1	51.06814	76.82867	29.50044		
			Right Occipital Pole (ROP)	46.65777	97.33313	29.24419	B-G	6.9976	48.92	-31								
			Left Occipital Pole (LOP)	57.8053	97.33276	30.41848												
							(L2)d=B onto L1 - B	-3.247	4.12	21.3	t (RFP)	0.993096	RFP onto L2	51.09055	76.80022	29.35337	Vertical frontal	-0.55996
							RFP-B	-8.265	-45.9	30.05	t (LFP)	0.967573	LFP onto L2	51.17341	76.69506	28.80965	Vertical occipital	-0.50943
							LFP-B	-2.195	-45.5	30.34	t (ROP)	1.193923	ROP onto L2	50.43855	77.62769	33.63163		
							ROP-B	-7.657	24.62	21.05	t (LOP)	1.170704	LOP onto L2	50.51394	77.53201	33.13698		
							LOP-B	3.4906	24.62	22.22								
							N of Plain	-1642	68.02	-263	RFP to P	1.522904					Lateral frontal	-2.97431
											LFP to P	4.497217					Lateral occipital	-0.72414
											ROP to P	5.229661						
											LOP to P	5.953805						
41462	Infant	F	Glabella(G)	40.54692	67.91141	41.60899	(L1)d=I - G	4.4358	-58.9	-30.8	t (RFP)	0.018412	RFP onto L1	40.62859	66.82784	41.0419	Antero-posterior frontal	0.085163
			Inion (I)	44.98272	9.059019	10.80834	RFP-G	3.7878	-4.61	6.701	t (LFP)	0.019691	LFP onto L1	40.63427	66.75256	41.0025	Antero-posterior occipital	-0.40729
			Basion (B)	45.48253	41.85892	5.87274	LFP-G	-2.821	-5.22	6.733	t (ROP)	1.001359	ROP onto L1	44.98875	8.979047	10.76649		
			Right Frontal Pole (RFP)	44.33475	63.30339	48.31	ROP-G	9.9403	-60.7	-26.8	t (LOP)	1.007477	LOP onto L1	45.01589	8.618989	10.57805		
			Left Frontal Pole (LFP)	37.72583	62.6922	48.34197	LOP-G	-0.047	-61.6	-27.3	t (B)	0.599248	B onto L1	43.20507	32.64422	23.15175		
			Right Occipital Pole (ROP)	50.48719	7.257629	14.84755	B-G	4.9356	-26.1	-35.7								
			Left Occipital Pole (LOP)	40.50027	6.320389	14.31978												
							(L2)d=B onto L1 - B	-2.277	-9.21	17.28	t (RFP)	1.384967	RFP onto L2	42.32832	29.09687	29.8036	Vertical frontal	1.077172
							RFP-B	-1.148	21.44	42.44	t (LFP)	1.439605	LFP onto L2	42.20388	28.59339	30.7477	Vertical occipital	1.129212
							LFP-B	-7.757	20.83	42.47	t (ROP)	1.190028	ROP onto L2	42.77228	30.89317	26.43525		
							ROP-B	5.0047	-34.6	8.975	t (LOP)	1.247306	LOP onto L2	42.64184	30.36537	27.42496		
							LOP-B	-4.982	-35.5	8.447								
							N of Plain	1300.7	6.499	174.9	RFP to P	4.624205					Lateral frontal	2.699764
											LFP to P	1.924441					Lateral occipital	1.996684
											ROP to P	5.984686						
											LOP to P	3.988002						
41466	Infant	F	Glabella(G)	41.38678	65.81852	41.79888	(L1)d=I - G	1.4718	-53	-34.3	t (RFP)	0.005329	RFP onto L1	41.39462	65.53619	41.61631	Antero-posterior frontal	0.14519
			Inion (I)	42.85857	12.83402	7.535573	RFP-G	1.6638	-1.17	1.267	t (LFP)	0.007629	LFP onto L1	41.39801	65.41431	41.53749	Antero-posterior occipital	-0.57149
			Basion (B)	42.97631	41.15129	5.710551	LFP-G	-2.531	-1.57	1.439	t (ROP)	1.035415	ROP onto L1	42.91069	10.95755	6.322122		
			Right Frontal Pole (RFP)	43.05061	64.64492	43.0657	ROP-G	5.8534	-60.1	-27.2	t (LOP)	1.04447	LOP onto L1	42.92402	10.4778	6.011879		
			Left Frontal Pole (LFP)	38.85555	64.24394	43.23812	LOP-G	-3.651	-60.3	-28.4	t (B)	0.639093	B onto L1	42.32739	31.95649	19.90144		
			Right Occipital Pole (ROP)	47.24021	5.744659	14.56927	B-G	1.5895	-24.7	-36.1								
			Left Occipital Pole (LOP)	37.73553	5.560303	13.39338												
							(L2)d=B onto L1 - B	-0.649	-9.19	14.19	t (RFP)	1.096696	RFP onto L2	42.26464	31.06739	21.27364	Vertical frontal	0.523348
							RFP-B	0.0743	23.49	37.36	t (LFP)	1.127623	LFP onto L2	42.24457	30.78302	21.71253	Vertical occipital	-0.52146
							LFP-B	-4.121	23.09	37.53	t (ROP)	1.566294	ROP onto L2	41.95991	26.74953	27.93765		
							ROP-B	4.2639	-35.4	8.859	t (LOP)	1.535478	LOP onto L2	41.97991	27.03288	27.50034		
							LOP-B	-5.241	-35.6	7.683								
							N of Plain	1066.9	-1.35	47.92	RFP to P	1.720469					Lateral frontal	-0.74165
											LFP to P	2.462119					Lateral occipital	-0.14415
											ROP to P	4.701737						
											LOP to P	4.845885						
41467	Juv2	M	Glabella(G)	52.947	74.99161	45.7542	(L1)d=I - G	-6.127	-66.3	-30.6	t (RFP)	0.040564	RFP onto L1	52.69846	72.30085	44.51148	Antero-posterior frontal	0.691479
			Inion (I)	46.8198	8.658001	15.1182	RFP-G	1.5442	-5.36	4.168	t (LFP)	0.049995	LFP onto L1	52.64068	71.67529	44.22257	Antero-posterior occipital	-0.51965
			Basion (B)	49.6836	35.0982	5.3946	LFP-G	-5.575	-5.84	4.978	t (ROP)	1.002694	ROP onto L1	46.8033	8.479308	15.03567		
			Right Frontal Pole (RFP)	54.49116	69.63638	49.92212	ROP-G	-0.041	-73.5	-16.8	t (LOP)	1.009781	LOP onto L1	46.75987	8.009191	14.81855		
			Left Frontal Pole (LFP)	47.37236	69.15546	50.7322	LOP-G	-10.22	-72.8	-17.5	t (B)	0.725919	B onto L1	48.49915	26.83878	23.51494		
			Right Occipital Pole (ROP)	52.90617	1.501404	28.92378	B-G	-3.263	-39.9	-40.4								
			Left Occipital Pole (LOP)	42.72888	2.178444	28.24958												
							(L2)d=B onto L1 - B	-1.184	-8.26	18.12	t (RFP)	1.296321	RFP onto L2	48.14817	24.39133	28.88438	Vertical frontal	1.357597
							RFP-B	4.8076	34.54	44.53	t (LFP)	1.364374	LFP onto L2	48.06757	23.82926	30.11753	Vertical occipital	-0.28844
							LFP-B	-2.311	34.06	45.34	t (ROP)	1.759011	ROP onto L2	47.60014	20.56978	37.26849		
							ROP-B	3.2226	-33.6	23.53	t (LOP)	1.744553	LOP onto L2	47.61726	20.6892	37.00649		
							LOP-B	-6.955	-32.9	22.85								
							N of Plain	1455	-147	27.96	RFP to P	2.155033					Lateral frontal	-2.70731
											LFP to P	4.862347					Lateral occipital	3.873191
											ROP to P	7.038971						
											LOP to P	3.16578						
41470	Infant	M	Glabella(G)	38.7612	13.1868	31.968	(L1)d=I - G	1.332	63.14	-10.4	t (RFP)	0.011681	RFP onto L1	38.77675	13.92427	31.84665	Antero-posterior frontal	0.759119
			Inion (I)	40.0932	76.32359	21.5784	RFP-G	-2.191	1.246	2.684	t (LFP)	0.023542	LFP onto L1	38.79255	14.67315	31.72341	Antero-posterior occipital	-0.09444
			Basion (B)	41.1588	45.5544	3.0636	LFP-G	2.6464	2.099	3.812	t (ROP)	1.001727	ROP onto L1	40.0955	76.43261	21.56046		
			Right Frontal Pole (RFP)	36.57051	14.43242	34.6518	ROP-G	-3.908	63.2	-11.3	t (LOP)	1.003202	LOP onto L1	40.09746	76.52578	21.54513		
			Left Frontal Pole (LFP)	41.40762	15.28548	35.77975	LOP-G	6.2169	63.2	-10.6	t (B)	0.573023	B onto L1	39.52446	49.36561	26.01453		
			Right Occipital Pole (ROP)	34.85292	76.3902	20.63061	B-G	2.3976	32.37	-28.9								
			Left Occipital Pole (LOP)	44.97805	76.3902	21.34694												
							(L2)d=B onto L1 - B	-1.634	3.811	22.95	t (RFP)	1.128549	RFP onto L2	39.31437	49.85554	28.96485	Vertical frontal	0.910411

							RFP-B	-4.588	-31.1	31.59	t (LFP)	1.167585	LFP onto L2	39.25057	50.00432	29.86076	Vertical occipital	-0.0046
							LFP-B	0.2488	-30.3	32.72	t (ROP)	0.976221	ROP onto L2	39.56333	49.27499	25.46877		
							ROP-B	-6.306	30.84	17.57	t (LOP)	0.976023	LOP onto L2	39.56365	49.27423	25.46424		
							LOP-B	3.8193	30.84	18.28								
							N of Plain	-1489	13.59	-108	RFP to P	2.001506					Lateral frontal	-0.8952
											LFP to P	2.896702					Lateral occipital	0.441218
											ROP to P	5.295611						
											LOP to P	4.854394						
41473	Juv2	F	Glabella(G)	48.91709	20.39323	36.85442	(L1)d=I - G	0.2666	74.38	-8.73	t (RFP)	0.035541	RFP onto L1	48.92656	23.0366	36.54414	Antero-posterior frontal	0.180386
			Inion (I)	49.18367	94.76853	28.12399	RFP-G	-2.583	3.101	3.513	t (LFP)	0.03795	LFP onto L1	48.9272	23.21575	36.52311	Antero-posterior occipital	0.019666
			Basion (B)	46.85111	66.84447	6.531164	LFP-G	3.0864	3.23	3.236	t (ROP)	0.99784	ROP onto L1	49.18309	94.60787	28.14285		
			Right Frontal Pole (RFP)	46.33365	23.49463	40.367	ROP-G	-5.779	74.73	-4.49	t (LOP)	0.997577	LOP onto L1	49.18302	94.58834	28.14514		
			Left Frontal Pole (LFP)	52.00349	23.62345	40.09023	LOP-G	4.8257	74.61	-5.07	t (B)	0.663164	B onto L1	49.09387	69.71627	31.06471		
			Right Occipital Pole (ROP)	43.13831	95.12476	32.36168	B-G	-2.066	46.45	-30.3								
			Left Occipital Pole (LOP)	53.74278	94.99863	31.77973												
							(L2)d=B onto L1 - B	2.2428	2.872	24.53	t (RFP)	1.145144	RFP onto L2	49.4194	70.13309	34.62561	Vertical frontal	0.253838
							RFP-B	-0.517	-43.3	33.84	t (LFP)	1.155378	LFP onto L2	49.44235	70.16248	34.8767	Vertical occipital	0.368659
							LFP-B	5.1524	-43.2	33.56	t (ROP)	1.148626	ROP onto L2	49.42721	70.14309	34.71102		
							ROP-B	-3.713	28.28	25.83	t (LOP)	1.163489	LOP onto L2	49.46054	70.18578	35.07568		
							LOP-B	6.8917	28.15	25.25								
							N of Plain	-1850	26.12	166	RFP to P	2.930461					Lateral frontal	0.191414
											LFP to P	2.739047					Lateral occipital	2.194028
											ROP to P	6.404394						
											LOP to P	4.210366						
41482	Infant	F	Glabella(G)	42.8944	71.38	33.6648	(L1)d=I - G	-1.859	-65.1	-13.5	t (RFP)	-0.00159	RFP onto L1	42.89736	71.48374	33.68627	Antero-posterior frontal	-0.01131
			Inion (I)	41.0352	6.2416	20.1856	RFP-G	3.2619	-0.38	1.888	t (LFP)	0.001423	LFP onto L1	42.89176	71.28735	33.64563	Antero-posterior occipital	-0.53861
			Basion (B)	42.164	29.6144	7.3704	LFP-G	-3.1	-0.3	1.404	t (ROP)	1.028109	ROP onto L1	40.98294	4.410655	19.80672		
			Right Frontal Pole (RFP)	46.15629	71.00441	35.55311	ROP-G	2.9808	-69.6	-1.72	t (LOP)	1.036203	LOP onto L1	40.96789	3.883426	19.69762		
			Left Frontal Pole (LFP)	39.79471	71.08119	35.06905	LOP-G	-7.568	-69.6	-2.93	t (B)	0.69472	B onto L1	41.60278	26.12704	24.30053		
			Right Occipital Pole (ROP)	45.87522	1.75989	31.94178	B-G	-0.73	-41.8	-26.3								
			Left Occipital Pole (LOP)	35.32605	1.7596	30.73922												
							(L2)d=B onto L1 - B	-0.561	-3.49	16.93	t (RFP)	1.105142	RFP onto L2	41.54377	25.76037	26.08059	Vertical frontal	-0.28291
							RFP-B	3.9923	41.39	28.18	t (LFP)	1.088784	LFP onto L2	41.55295	25.81742	25.80365	Vertical occipital	-0.83482
							LFP-B	-2.369	41.47	27.7	t (ROP)	1.7086	ROP onto L2	41.20509	23.65589	36.29722		
							ROP-B	3.7112	-27.9	24.57	t (LOP)	1.66033	LOP onto L2	41.23219	23.82423	35.48		
							LOP-B	-6.838	-27.9	23.37								
							N of Plain	1149.8	-39	30.07	RFP to P	3.320984					Lateral frontal	0.270965
											LFP to P	3.050019					Lateral occipital	0.01872
											ROP to P	5.294815						
											LOP to P	5.276095						
41488	Juv1	F	Glabella(G)	42.496	74.03601	35.5904	(L1)d=I - G	1.328	-70.8	-0.13	t (RFP)	0.017045	RFP onto L1	42.51864	72.82842	35.58814	Antero-posterior frontal	-0.19767
			Inion (I)	43.82401	3.1872	35.4576	RFP-G	2.4047	-1.17	1.438	t (LFP)	0.014255	LFP onto L1	42.51493	73.02605	35.58851	Antero-posterior occipital	0.178769
			Basion (B)	44.488	30.0792	11.288	LFP-G	-1.547	-1.04	-0.5	t (ROP)	1.010761	ROP onto L1	43.8383	2.424829	35.45617		
			Right Frontal Pole (RFP)	44.90075	72.87037	37.02837	ROP-G	8.2727	-71.5	-1.18	t (LOP)	1.008238	LOP onto L1	43.83494	2.603566	35.45651		
			Left Frontal Pole (LFP)	40.94941	72.99764	35.08939	LOP-G	-7.339	-71.6	-1.79	t (B)	0.621381	B onto L1	43.3212	30.01193	35.50788		
			Right Occipital Pole (ROP)	50.76866	2.556702	34.40609	B-G	1.992	-44	-24.3								
			Left Occipital Pole (LOP)	35.15729	2.444014	33.80112												
							(L2)d=B onto L1 - B	-1.167	-0.07	24.22	t (RFP)	1.054595	RFP onto L2	43.2575	30.00826	36.83016	Vertical frontal	-1.74694
							RFP-B	0.4127	42.79	25.74	t (LFP)	0.98255	LFP onto L2	43.34156	30.01311	35.08524	Vertical occipital	0.147254
							LFP-B	-3.539	42.92	23.8	t (ROP)	0.942976	ROP onto L2	43.38773	30.01577	34.12677		
							ROP-B	6.2807	-27.5	23.12	t (LOP)	0.949049	LOP onto L2	43.38065	30.01536	34.27386		
							LOP-B	-9.331	-27.6	22.51								
							N of Plain	1716	32.01	82.76	RFP to P	2.449081					Lateral frontal	0.861081
											LFP to P	1.587999					Lateral occipital	-1.87578
											ROP to P	6.872997						
											LOP to P	8.748776						
41497	Juv2	F	Glabella(G)	27.75475	48.4193	43.632	(L1)d=I - G	69.872	11.45	-26.1	t (RFP)	0.061572	RFP onto L1	32.05685	49.12451	42.02757	Antero-posterior frontal	0.143271
			Inion (I)	97.6264	59.87268	17.574	RFP-G	5.7841	5.372	4.421	t (LFP)	0.063471	LFP onto L1	32.18954	49.14626	41.97808	Antero-posterior occipital	-1.10244
			Basion (B)	67.02346	56.84269	5.6358	LFP-G	7.3283	-1.7	5.036	t (ROP)	0.976146	ROP onto L1	95.9597	59.59947	18.19558		
			Right Frontal Pole (RFP)	33.53889	53.79105	48.05258	ROP-G	70.319	17.19	-17.1	t (LOP)	0.990758	LOP onto L1	96.98068	59.76683	17.81482		
			Left Frontal Pole (LFP)	35.08302	46.7159	48.66842	LOP-G	72.656	5.146	-19.3	t (B)	0.672907	B onto L1	74.77185	56.12636	26.0974		
			Right Occipital Pole (ROP)	98.07422	65.60741	26.50613	B-G	39.269	8.423	-38								
			Left Occipital Pole (LOP)	100.4104	53.56537	24.28554												
							(L2)d=B onto L1 - B	7.7484	-0.72	20.46	t (RFP)	1.274237	RFP onto L2	76.89674	55.92991	31.70873	Vertical frontal	1.353684
							RFP-B	-33.48	-3.05	42.42	t (LFP)	1.336074	LFP onto L2	77.37588	55.88562	32.974	Vertical occipital	-0.85463
							LFP-B	-31.94	-10.1	43.03	t (ROP)	1.380044	ROP onto L2	77.71658	55.85412	33.8737		
							ROP-B	31.051	8.765	20.87	t (LOP)	1.341004	LOP onto L2	77.41408	55.88209	33.07489		
							LOP-B	33.387	-3.28	18.65								
							N of Plain	-215.7	1632	138.8	RFP to P	4.922704					Lateral frontal	2.706198
											LFP to P	2.216506					Lateral occipital	0.326946
											ROP to P	6.357293						
											LOP to P	6.030347						
41499	Subadult	M	Glabella(G)	57.821	77.318	39.865	(L1)d=I - G	-0.804	-74	-13.9	t (RFP)	0.050976	RFP onto L1	57.78001	73.5474	39.15801	Antero-posterior frontal	0.549971
			Inion (I)	57.017	3.35	25.996	RFP-G	2.4743	-4.35	2.226	t (LFP)	0.058284	LFP onto L1	57.77414	73.00688	39.05667	Antero-posterior occipital	-0.55902
			Basion (B)	54.471	27.001	3.953	LFP-G	-4.156	-4.79	1.961	t (ROP)	0.982459	ROP onto L1	57.0311	4.647493	26.23928		
			Right Frontal Pole (RFP)	60.29531	72.97014	42.09095	ROP-G	7.3374	-74.1	-6.64	t (LOP)	0.989886	LOP onto L1	57.02513	4.098078	26.13626		
			Left Frontal Pole (LFP)	53.66499	72.5323	41.82602	LOP-G	-6.606	-74.9	-4.69	t (B)	0.745482	B onto L1	57.22163	22.17618	29.52591		
			Right Occipital Pole (ROP)	65.15842	3.250053	33.22114	B-G	-3.35	-50.3	-35.9								
			Left Occipital Pole (LOP)	51.2152	2.467239	35.17088												
							(L2)d=B onto L1 - B	2.7506	-4.82	25.57	t (RFP)	1.123693	RFP onto L2	57.56187	21.57938	32.68911	Vertical frontal	-0.87508
							RFP-B	5.8243	45.97	38.14	t (LFP)	1.090254	LFP onto L2	57.46989	21.74072	31.83396	Vertical occipital	0.584078
							LFP-B	-0.806	45.53	37.87	t (ROP)	1.30321	ROP onto L2	58.05565	20.71324	37.27988		
							ROP-B	10.687	-23.8	29.27	t (LOP)	1.32553	LOP onto L2	58.11704	20.60556	37.85066		
							LOP-B	-3.256	-24.5	31.22								
							N of Plain	1958.5	17.59	-207	RFP to P	2.1873					Lateral frontal	-2.19463
											LFP to P	4.381925					Lateral occipital	0.591265
											ROP to P	7.334344						
											LOP to P	6.743079						
41529	Adult	M	Glabella(G)	54.1458	77.72221	50.8824	(L1)d=I - G	2.2644	-75.9	-29.2	t (RFP)	0.0799	RFP onto L1	54.32673	71.66119	48.55165	Antero-posterior frontal	-0.18413
			Inion (I)	56.4102	1.8648	21.7116	RFP-G	5.4163	-7.01	0.547	t (LFP)	0.077635	LFP onto L1	54.3216	71.83298	48.61771	Antero-posterior occipital	0.19018
			Basion (B)	56.5434	31.7016	3.663	LFP-G	-3.016	-6.42	-1.13	t (ROP)	0.977783	ROP onto L1	56.35989	3.550151	22.3597		
			Right Frontal Pole (RFP)	59.56208	70.71065	51.42988	ROP-G	7.9369	-74.7	-26.7	t (LOP)	0.975444	LOP onto L1	56.3546	3.72759	22.42793		
			Left Frontal Pole (LFP)	51.1298	71.30076	49.75397	LOP-G	-3.769	-75.1	-26.1	t (B)	0.737301	B onto L1	55.81535	21.79248	29.37474		
			Right Occipital Pole (ROP)	62.08267	3.037155	24.13795	B-G	2.3976	-46	-47.2								
			Left Occipital Pole (LOP)	50.37658	2.628731	24.82142												
							(L2)d=B onto L1 - B	-0.728	-9.91	25.71	t (RFP)	1.104778	RFP onto L2	55.73906	20.75422	32.06876	Vertical frontal	-1.55266
							RFP-B	3.0187	39.01	47.77	t (LFP)	1.04845	LFP onto L2	55.78007	21.31238	30.62048	Vertical occipital	1.093531
							LFP-B	-5.414	39.6	46.09	t (ROP)	1.061382	ROP onto L2	55.77066	21.18423	30.95298		
							ROP-B	5.5393	-28.7	20.47	t (LOP)	1.101053	LOP onto L2	55.74177	20.79113	31.973		
							LOP-B	-6.167	-29.1	21.16								
							N of Plain	2239.5	36.98	77.67	RFP to P	5.315558					Lateral frontal	2.156704
											LFP to P	3.158854					Lateral occipital	-0.13708
											ROP to P	5.771722						
											LOP to P	5.908799						
41535	Juv2	F	Glabella(G)	51.20427	73.57701	40.35082	(L1)d=I - G	-4.328	-70	-17.1	t (RFP)	0.034735	RFP onto L1	51.05393	71.14621	39.75642	Antero-posterior frontal	0.499114
			Inion (I)	46.87621	3.595618	23.23834	RFP-G	3.7247	-3.25	1.779	t (LFP)	0.04165	LFP onto L1	51.024	70.66226	39.63808	Antero-posterior occipital	0.016991
			Basion (B)	46.87621	31.09544	4.328058	LFP-G	-4.229	-3.61	3.137	t (ROP)	0.998424	ROP onto L1	46.88303	3.705909	23.26531		
			Right Frontal Pole (RFP)	54.929	70.32629	42.12941	ROP-G	1.2074	-70.9	-14.1	t (LOP)	0.998189	LOP onto L1	46.88405	3.722383	23.26934		
			Left Frontal Pole (LFP)	46.97479	69.97141	43.48743	LOP-G	-8.613	-70.3	-14	t (B)	0.692669	B onto L1	48.20635	25.10304	28.49753		

			Right Occipital Pole (ROP)	52.41164	2.630131	26.26641	B-G	-4.328	-42.5	-36								
			Left Occipital Pole (LOP)	42.5914	3.229591	26.3703												
							(L2)d=B onto L1 - B	1.3301	-5.99	24.17	t (RFP)	1.108422	RFP onto L2	48.35057	24.45333	31.11804	Vertical frontal	0.977241
							RFP-B	8.0528	39.23	37.8	t (LFP)	1.147611	LFP onto L2	48.4027	24.2185	32.06521	Vertical occipital	-0.56718
							LFP-B	0.0986	38.88	39.16	t (ROP)	1.138838	ROP onto L2	48.39103	24.27107	31.85318		
							ROP-B	5.5354	-28.5	21.94	t (LOP)	1.116093	LOP onto L2	48.36077	24.40736	31.30345		
							LOP-B	-4.285	-27.9	22.04								
							N of Plain	1794	-81.8	-119	RFP to P	3.742927					Lateral frontal	-0.51637
											LFP to P	4.259292					Lateral occipital	0.899764
											ROP to P	5.36123						
											LOP to P	4.461466						
41537	Juv2	M	Glabella(G)	51.4862	26.2922	45.3492	(L1)d=I - G	-2.39	69.06	-30	t (RFP)	0.044065	RFP onto L1	51.38088	29.33522	44.02838	Antero-posterior frontal	0.432363
			Inion (I)	49.096	95.34961	15.3748	RFP-G	-3.104	5.147	3.766	t (LFP)	0.049805	LFP onto L1	51.36716	29.73163	43.85631	Antero-posterior occipital	-0.16972
			Basion (B)	48.8376	64.27701	5.2326	LFP-G	3.9566	5.708	3.41	t (ROP)	0.981572	ROP onto L1	49.14005	94.07702	15.92717		
			Right Frontal Pole (RFP)	48.38268	31.43958	49.11565	ROP-G	-7.855	70.58	-22.6	t (LOP)	0.983825	LOP onto L1	49.13467	94.23263	15.85963		
			Left Frontal Pole (LFP)	55.44282	32.00059	48.75873	LOP-G	3.3212	71.29	-22.2	t (B)	0.675456	B onto L1	49.87173	72.93747	25.1028		
			Right Occipital Pole (ROP)	43.63147	96.86732	22.79495	B-G	-2.649	37.98	-40.1								
			Left Occipital Pole (LOP)	54.8074	97.57829	23.11527												
							(L2)d=B onto L1 - B	1.0341	8.66	19.87	t (RFP)	1.246782	RFP onto L2	50.12693	75.07472	30.00641	Vertical frontal	0.233531
							RFP-B	-0.455	-32.8	43.88	t (LFP)	1.257544	LFP onto L2	50.13806	75.16792	30.22025	Vertical occipital	1.10964
							LFP-B	6.6052	-32.3	43.53	t (ROP)	1.329016	ROP onto L2	50.21197	75.7869	31.64042		
							ROP-B	-5.206	32.59	17.56	t (LOP)	1.380151	LOP onto L2	50.26485	76.22976	32.65648		
							LOP-B	5.9698	33.3	17.88								
							N of Plain	-1632	-16.5	92.11	RFP to P	3.258744					Lateral frontal	-0.55685
											LFP to P	3.81559					Lateral occipital	0.570149
											ROP to P	5.858435						
											LOP to P	5.288286						
41544	Infant	M	Glabella(G)	39.2392	8.007999	30.0608	(L1)d=I - G	0.7392	60.12	-14.2	t (RFP)	0.013759	RFP onto L1	39.24937	8.835188	29.86587	Antero-posterior frontal	-0.46581
			Inion (I)	39.9784	68.12959	15.8928	RFP-G	-1.233	0.647	-1.02	t (LFP)	0.006218	LFP onto L1	39.24379	8.381828	29.97271	Antero-posterior occipital	0.085386
			Basion (B)	40.5944	45.5224	4.9896	LFP-G	1.1135	0.633	1.071	t (ROP)	1.048114	ROP onto L1	40.01396	71.02228	15.21112		
			Right Frontal Pole (RFP)	38.00597	8.655211	29.03727	ROP-G	-6.595	63.98	-11.1	t (LOP)	1.046732	LOP onto L1	40.01294	70.93918	15.23071		
			Left Frontal Pole (LFP)	40.3527	8.641371	31.13193	LOP-G	6.3049	63.98	-10.1	t (B)	0.684412	B onto L1	39.74511	49.15592	20.36406		
			Right Occipital Pole (ROP)	32.64419	71.98711	18.92082	B-G	1.3552	37.51	-25.1								
			Left Occipital Pole (LOP)	45.54411	71.98492	19.95689												
							(L2)d=B onto L1 - B	-0.849	3.634	15.37	t (RFP)	0.95071	RFP onto L2	39.78698	48.97682	19.60625	Vertical frontal	1.906406
							RFP-B	-2.588	-36.9	24.05	t (LFP)	1.07121	LFP onto L2	39.68464	49.41466	21.45887	Vertical occipital	0.313846
							LFP-B	-0.242	-36.9	26.14	t (ROP)	1.26688	ROP onto L2	39.51846	50.12563	24.46719		
							ROP-B	-7.95	26.46	13.93	t (LOP)	1.286717	LOP onto L2	39.50161	50.19771	24.77218		
							LOP-B	4.9497	26.46	14.97								
							N of Plain	-975.8	-0.67	-53.7	RFP to P	1.287203					Lateral frontal	0.116051
											LFP to P	1.171152					Lateral occipital	1.37052
											ROP to P	7.153943						
											LOP to P	5.783422						
41549	Juv1	M	Glabella(G)	47.9085	74.78399	35.547	(L1)d=I - G	-0.184	-70.2	-14.8	t (RFP)	0.039772	RFP onto L1	47.90116	71.99312	34.95752	Antero-posterior frontal	-0.27318
			Inion (I)	47.724	4.6125	20.7255	RFP-G	2.7316	-3.96	4.908	t (LFP)	0.035963	LFP onto L1	47.90186	72.2604	35.01397	Antero-posterior occipital	-0.72504
			Basion (B)	48.831	32.595	3.7515	LFP-G	-4.116	-3.59	4.55	t (ROP)	0.999045	ROP onto L1	47.72418	4.679524	20.73966		
			Right Frontal Pole (RFP)	50.64008	70.82474	40.45505	ROP-G	6.5853	-71.3	-9.2	t (LOP)	1.009154	LOP onto L1	47.72231	3.970142	20.58982		
			Left Frontal Pole (LFP)	43.79288	71.19752	40.09726	LOP-G	-8.282	-71.9	-9.93	t (B)	0.66713	B onto L1	47.78541	27.97046	25.65913		
			Right Occipital Pole (ROP)	54.4938	3.477524	26.34619	B-G	0.9225	-42.2	-31.8								
			Left Occipital Pole (LOP)	39.62614	2.928764	25.62094												
							(L2)d=B onto L1 - B	-1.046	-4.62	21.91	t (RFP)	1.244768	RFP onto L2	47.52949	26.83851	31.02142	Vertical frontal	-0.1072
							RFP-B	1.8091	38.23	36.7	t (LFP)	1.239986	LFP onto L2	47.53449	26.86063	30.91664	Vertical occipital	0.097914
							LFP-B	-5.038	38.6	36.35	t (ROP)	1.241442	ROP onto L2	47.53296	26.8539	30.94855		
							ROP-B	5.6628	-29.1	22.59	t (LOP)	1.24581	LOP onto L2	47.5284	26.83369	31.04425		
							LOP-B	-9.205	-29.7	21.87								
							N of Plain	1605.8	-19.5	72.52	RFP to P	2.99812					Lateral frontal	-0.86416
											LFP to P	3.862276					Lateral occipital	-0.81797
											ROP to P	7.029746						
											LOP to P	7.847719						
41550	Juv2	F	Glabella(G)	50.4526	25.0002	37.2742	(L1)d=I - G	1.5504	73.71	-13.5	t (RFP)	0.052631	RFP onto L1	50.5342	28.87959	36.5636	Antero-posterior frontal	0.82418
			Inion (I)	52.003	98.70881	23.7728	RFP-G	-1.536	4.647	3.295	t (LFP)	0.063628	LFP onto L1	50.55125	29.69011	36.41513	Antero-posterior occipital	0.486533
			Basion (B)	52.1322	72.35201	5.2326	LFP-G	4.6982	5.452	3.828	t (ROP)	0.981641	ROP onto L1	51.97454	97.35559	24.02067		
			Right Frontal Pole (RFP)	48.91654	29.64732	40.5691	ROP-G	-3.257	74.24	-3.52	t (LOP)	0.97515	LOP onto L1	51.96447	96.87712	24.10831		
			Left Frontal Pole (LFP)	55.15085	30.45181	41.1017	LOP-G	9.807	73.44	-3.69	t (B)	0.69877	B onto L1	51.53598	76.50557	27.83983		
			Right Occipital Pole (ROP)	47.19511	99.23953	33.7569	B-G	1.6796	47.35	-32								
			Left Occipital Pole (LOP)	60.2596	98.43899	33.5876												
							(L2)d=B onto L1 - B	-0.596	4.154	22.61	t (RFP)	1.179133	RFP onto L2	51.42917	77.24961	31.88952	Vertical frontal	0.507328
							RFP-B	-3.216	-42.7	35.34	t (LFP)	1.201197	LFP onto L2	51.41602	77.34126	32.38833	Vertical occipital	-0.64983
							LFP-B	3.0186	-41.9	35.87	t (ROP)	1.436516	ROP onto L2	51.27571	78.31867	37.70825		
							ROP-B	-4.937	26.89	28.52	t (LOP)	1.408255	LOP onto L2	51.29256	78.20128	37.06933		
							LOP-B	8.1274	26.09	28.36								
							N of Plain	-1722	27	-50.4	RFP to P	1.511692					Lateral frontal	-3.21046
											LFP to P	4.722155					Lateral occipital	-4.02159
											ROP to P	4.52165						
											LOP to P	8.543237						

3. Data Compression: Petalial components; Size correction of petalial components

Id number	ECV	Sex	Antero-posterior frontal	Antero-posterior occipital	Vertical frontal	Vertical occipital	Lateral frontal	Lateral occipital
41413	108689	M	0.564858251	-0.485621723	-0.863837311	-1.535312039	-2.510143346	1.684713258
41415	102076	M	0.172271943	-1.394266336	-0.23906566	-2.422567049	-0.080077662	-3.374934405
41422	104821	F	0.091423701	0.056598711	0.222400043	-4.174350929	-1.833332935	-0.432102847
41425	103532	F	0.057194441	0.046091514	-0.572689996	-1.211314266	0.005226747	0.395045665
41428	103517	M	-0.140106188	-0.758741076	0.044334912	-1.672639822	-0.365004	4.518775136
41431	101762	M	0.371724684	0.781156199	2.925101407	6.75394614	-1.91693478	-5.552523917
41437	965754	F	0.290763556	-0.001754365	0.285094999	-0.244265425	-0.408142564	0.397404186
41438	85961	F	0.450898249	0.654648683	1.368735063	2.241880071	-0.079981079	0.182312457
41447	103864	M	0.142936111	0.111461433	-0.602314796	2.3649948	0.025939643	-1.356816003
41461	994936	M	0.689388493	-0.562887545	-0.559960415	-0.509426693	-2.974313206	-0.724143819
41462	99606.4	F	0.085162608	-0.407291607	1.077171949	1.1292119	2.699763812	1.996683943
41466	84891.8	F	0.145190332	-0.571485764	0.52334825	-0.521463777	-0.741649214	-0.144148463
41467	111262	M	0.691478596	-0.519652052	1.357596777	-0.288438092	-2.707314133	3.873191224
41470	72392	M	0.759119197	-0.09444208	0.910411397	-0.004603062	-0.895195849	0.441217853
41473	106639	F	0.180385504	0.019665535	0.253838062	0.368658744	0.191413705	2.194028344
41482	102418	F	-0.011311024	-0.53860846	-0.282907662	-0.834820481	0.27096509	0.018719551
41488	105454	F	-0.19766867	0.178768549	-1.746943163	0.147254426	0.861081181	-1.875779103
41497	95755.7	F	0.143270873	-1.10244488	1.353684016	-0.854633962	2.706197559	0.326946021
41499	97544	M	0.549970663	-0.559020923	-0.875082857	0.584078434	-2.194625436	0.591264924
41529	101465	M	-0.184133992	0.190179814	-1.552660989	1.093530998	2.156704435	-0.137076724
41535	94282	F	0.499114299	0.016990527	0.977241308	-0.567182388	-0.51636529	0.899763661
41537	92666.7	M	0.432363228	-0.169715034	0.233531437	1.109640472	-0.556846015	0.570148758
41544	85825.2	M	-0.465811651	0.085385718	1.906406482	0.313846448	0.116050523	1.370520455
41549	91862	M	-0.273177424	-0.725036353	-0.107201169	0.097913986	-0.864156385	-0.817972937
41550	89522.7	F	0.824180073	0.486533017	0.507327967	-0.649832567	-3.21046334	-4.021587567

Size correction: (X/ECV^(1/3))*100

Antero-posterior frontal	Antero-posterior occipital	Vertical frontal	Vertical occipital	Lateral frontal	Lateral occipital
1.183616323	-1.017582371	-1.810103579	-3.217126398	-5.259809223	3.530184978
0.368615283	-2.983352202	-0.511535741	-5.183637123	-0.1713445	-7.221445232
0.193899207	0.120039388	0.471685038	-8.853320579	-3.888289336	-0.916440685
0.121804207	0.098158845	-1.219629898	-2.579676797	0.011131148	0.841309448
-0.298391713	-1.615931836	0.094422456	-3.562311337	-0.777368726	9.623879383
0.796207363	1.673180028	6.26535546	14.4664637	-4.105935528	-11.89310427
0.294160575	-0.001774861	0.288425792	-0.247119202	-0.412910934	0.402047098
1.021671775	1.483341494	3.101360417	5.079783736	-0.181225834	0.413094289
0.304079363	0.237120776	-1.281352195	5.031241634	0.055183468	-2.886462652
0.690556125	-0.56384092	-0.560908832	-0.51028952	-2.979350864	-0.725370317
0.183718633	-0.878637455	2.323749383	2.436013542	5.824116099	4.307383871
0.330356191	-1.300319781	1.190790959	-1.186503159	-1.687498104	-0.327985594
1.437682944	-1.080430973	2.822637958	-0.599704066	-5.628893472	8.052918769
1.821432645	-0.226604581	2.184443556	-0.0110446	-2.14793533	1.058659303
0.380390458	0.041469973	0.535284566	0.777414288	0.40364633	4.626687985
-0.024175557	-1.151191941	-0.604671193	-1.784299135	0.5791458	0.040010134
-0.418392112	0.378387485	-3.697638269	0.311683638	1.822593198	-3.970336724
0.313162459	-2.409731602	2.958891832	-1.868064792	5.915225238	0.714640862
1.19473798	-1.214398464	-1.9010009	1.268832567	-4.767531321	1.28444426
-0.394786125	0.407748463	-3.328929171	2.34454737	4.62400766	-0.293894617
1.096622326	0.03733051	2.147132707	-1.246177219	-1.13452511	1.976903729
0.955449018	-0.37504129	0.51606466	2.452116254	-1.230534753	1.259931546
-1.056019828	0.193573971	4.321925052	0.711506616	0.263092718	3.10704288
-0.605433116	-1.606871508	-0.237586025	0.21700318	-1.915198139	-1.812843455
1.842373673	1.087596814	1.134081885	-1.452636933	-7.176675744	-8.989864356

4. Spearman Correlation

Id number	ECV	ECV^1/3	Rank	Sex	Antero-posterior frontal	Absolute	Rank	Antero-posterior occipital	Absolute	Rank	Vertical frontal	Absolute	Rank	Vertical occipital	Absolute	Rank	Lateral frontal	Absolute	Rank	Lateral occipital	Absolute	Rank
41422	104821	34940.33	7	F	0.091424	0.091424	22	0.056599	0.056599	21	0.2224	0.2224	23	-4.17435	4.174351	2	-1.83333	1.833333	10	-0.4321	0.432103	18
41425	103532	34510.67	9	F	0.057194	0.057194	24	0.046092	0.046092	22	-0.57269	0.57269	14	-1.21131	1.211314	8	0.005227	0.005227	25	0.395046	0.395046	20
41437	965754	321918	2	F	0.290764	0.290764	12	-0.00175	0.001754	25	0.285095	0.285095	18	-0.24427	0.244265	22	-0.40814	0.408143	17	0.397404	0.397404	19
41438	85961	28653.67	22	F	0.450898	0.450898	9	0.654649	0.654649	6	1.368735	1.368735	5	2.24188	2.24188	5	-0.07998	0.079981	23	0.182312	0.182312	22
41462	99606.4	33202.13	15	F	0.085163	0.085163	23	-0.40729	0.407292	14	1.077172	1.077172	8	1.129212	1.129212	9	2.699764	2.699764	5	1.996684	1.996684	7
41466	84891.8	28297.27	24	F	0.14519	0.14519	18	-0.57149	0.571486	7	0.523348	0.523348	16	-0.52146	0.521464	17	-0.74165	0.741649	14	-0.14415	0.144148	23
41473	106639	35546.33	5	F	0.180386	0.180386	16	0.019666	0.019666	23	0.253838	0.253838	20	0.368659	0.368659	19	0.191414	0.191414	20	2.194028	2.194028	6
41482	102418	34139.33	11	F	-0.01131	0.011311	25	-0.53861	0.538608	10	-0.28291	0.282908	19	-0.83482	0.83482	13	0.270965	0.270965	19	0.01872	0.01872	25
41488	105454	35151.33	6	F	-0.19767	0.197669	14	0.178769	0.178769	16	-1.74694	1.746943	3	0.147254	0.147254	23	0.861081	0.861081	13	-1.87578	1.875779	8
41497	95755.7	31918.57	17	F	0.143271	0.143271	19	-1.10244	1.102445	2	1.353684	1.353684	7	-0.85463	0.854634	12	2.706198	2.706198	4	0.326946	0.326946	21
41535	94282	31427.33	18	F	0.499114	0.499114	7	0.016991	0.016991	24	0.977241	0.977241	9	-0.56718	0.567182	16	-0.51637	0.516365	16	0.899764	0.899764	12
41550	89522.7	29840.9	21	F	0.82418	0.82418	1	0.486533	0.486533	12	0.507328	0.507328	17	-0.64983	0.649833	14	-3.21046	3.210463	1	-4.02159	4.021588	3
41413	108689	36229.67	4	M	0.564858	0.564858	5	-0.48562	0.485622	13	-0.86384	0.863837	12	-1.53531	1.535312	7	-2.51014	2.510143	6	1.684713	1.684713	9
41415	102076	34025.33	12	M	0.172272	0.172272	17	-1.39427	1.394266	1	-0.23907	0.239066	21	-2.42257	2.422567	3	-0.08008	0.080078	22	-3.37493	3.374934	5
41428	103517	34505.67	10	M	-0.14011	0.140106	21	-0.75874	0.758741	4	0.044335	0.044335	25	-1.67264	1.67264	6	-0.365	0.365004	18	4.518775	4.518775	2
41431	101762	33920.67	13	M	0.371725	0.371725	11	0.781156	0.781156	3	2.925101	2.925101	1	6.753946	6.753946	1	-1.91693	1.916935	9	-5.55252	5.552524	1
41447	103864	34621.33	8	M	0.142936	0.142936	20	0.111461	0.111461	18	-0.60231	0.602315	13	2.364995	2.364995	4	0.02594	0.02594	24	-1.35682	1.356816	11
41461	994936	331645.3	1	M	0.689388	0.689388	4	-0.56289	0.562888	8	-0.55996	0.55996	15	-0.50943	0.509427	18	-2.97431	2.974313	2	-0.72414	0.724144	14
41467	111262	37087.33	3	M	0.691479	0.691479	3	-0.51965	0.519652	11	1.357597	1.357597	6	-0.28844	0.288438	21	-2.70731	2.707314	3	3.873191	3.873191	4
41470	72392	24130.67	25	M	0.759119	0.759119	2	-0.09444	0.094442	19	0.910411	0.910411	10	-0.0046	0.004603	25	-0.8952	0.895196	11	0.441218	0.441218	17
41499	97544	32514.67	16	M	0.549971	0.549971	6	-0.55902	0.559021	9	-0.87508	0.875083	11	0.584078	0.584078	15	-2.19463	2.194625	7	0.591265	0.591265	15
41529	101465	33821.67	14	M	-0.18413	0.184134	15	0.19018	0.19018	15	-1.55266	1.552661	4	1.093531	1.093531	11	2.156704	2.156704	8	-0.13708	0.137077	24
41537	92666.7	30888.9	19	M	0.432363	0.432363	10	-0.16972	0.169715	17	0.233531	0.233531	22	1.10964	1.10964	10	-0.55685	0.556846	15	0.570149	0.570149	16
41544	85825.2	28608.4	23	M	-0.46581	0.465812	8	0.085386	0.085386	20	1.906406	1.906406	2	0.313846	0.313846	20	0.116051	0.116051	21	1.37052	1.37052	10
41549	91862	30620.67	20	M	-0.27318	0.273177	13	-0.72504	0.725036	5	-0.1072	0.107201	24	0.097914	0.097914	24	-0.86416	0.864156	12	-0.81797	0.817973	13

	Antero-posterior frontal	Antero-posterior occipital	Vertical frontal	Vertical occipital	Lateral frontal	Lateral occipital
Spearman coefficient (F)	-0.34114	-0.68406	-0.3332	-0.27951	-0.28141	0.107111
Spearman coefficient (M)	-0.00783	0.32096	-0.02537	0.350412	0.379196	0.354746
Spearman coefficient (All)	-0.15923	-0.18538	-0.15154	0.091538	0.061538	0.220769
T statistic (F)	1.147617	2.965575	1.117531	0.920585	0.927391	0.340675
T statistic (M)	0.025971	1.123972	0.084159	1.240861	1.35916	1.258403
T statistic (All)	0.773513	0.904756	0.735244	0.440854	0.295689	1.085557
df (F)	10	10	10	10	10	10
df (M)	11	11	11	11	11	11
df (All)	23	23	23	23	23	23
p-value (F)	0.27784	0.014153	0.289897	0.37894	0.375565	0.740397
p-value (M)	0.979746	0.284955	0.934442	0.240469	0.201309	0.2343
p-value (All)	0.447097	0.374975	0.469622	0.663435	0.770121	0.288922

Spearman correlation table

alpha	0.1	0.05	0.025	0.01	0.005
n=12	0.406	0.503	0.587	0.678	0.727
n=13	0.385	0.484	0.56	0.648	0.703
n=25	0.265	0.337	0.398	0.466	0.511

5. Grubbs Test statistic: Size corrected petalial components sorted in ascending order; Grubbs test calculations

Two sided Grubbs test

	APF	Grubbs	APO	Grubbs	VF	Grubbs	VO	Grubbs	LF	Grubbs	LO	Grubbs
	-1.05602	2.070502	-2.98335	2.289135	-3.69764	1.856091	-8.85332	2.123533	-7.17668	1.887664	-11.8931	2.54352
	-0.60543	1.458879	-2.40973	1.775534	-3.32893	1.697151	-5.18364	1.254308	-5.62889	1.417787	-8.98986	1.927181
	-0.41839	1.204991	-1.61593	1.064791	-1.901	1.08161	-3.56231	0.870271	-5.25981	1.30574	-7.22145	1.551758
	-0.39479	1.172949	-1.60687	1.056678	-1.8101	1.042427	-3.21713	0.788508	-4.76753	1.156294	-3.97034	0.861569
	-0.29839	1.042104	-1.30032	0.782202	-1.28135	0.814497	-2.57968	0.637518	-4.10594	0.955447	-2.88646	0.63147
	-0.02418	0.669885	-1.2144	0.705271	-1.21963	0.78789	-1.86806	0.468961	-3.88829	0.889374	-1.81284	0.403548
	0.121804	0.471733	-1.15119	0.648678	-0.60467	0.522799	-1.7843	0.449119	-2.97935	0.613438	-0.91644	0.213248
	0.183719	0.387691	-1.08043	0.58532	-0.56091	0.503934	-1.45264	0.37056	-2.14794	0.361036	-0.72537	0.172685
	0.193899	0.373872	-1.01758	0.529048	-0.51154	0.482651	-1.24618	0.321656	-1.9152	0.290382	-0.32799	0.088323
	0.294161	0.237778	-0.87864	0.404641	-0.23759	0.364559	-1.1865	0.307522	-1.6875	0.221256	-0.29389	0.081085
	0.304079	0.224315	-0.56384	0.122782	0.094422	0.221439	-0.5997	0.168529	-1.23053	0.082531	0.04001	0.0102
	0.313162	0.211985	-0.37504	0.046263	0.288426	0.137809	-0.51029	0.147349	-1.13453	0.053385	0.402047	0.066658
	0.330356	0.188647	-0.2266	0.179168	0.471685	0.058812	-0.24712	0.085013	-0.77737	0.055041	0.413094	0.069004
	0.368615	0.136714	-0.00177	0.380474	0.516065	0.039681	-0.01104	0.029095	-0.41291	0.165683	0.714641	0.13302
	0.38039	0.120731	0.037331	0.415487	0.535285	0.031396	0.217003	0.024922	-0.18123	0.236019	0.841309	0.159911
	0.690556	0.300286	0.04147	0.419194	1.134082	0.226729	0.311684	0.047349	-0.17134	0.239018	1.058659	0.206053
	0.796207	0.443696	0.098159	0.469951	1.190791	0.251175	0.711507	0.142053	0.011131	0.294414	1.259932	0.248781
	0.955449	0.659849	0.120039	0.489542	2.147133	0.663427	0.777414	0.157665	0.055183	0.307788	1.284444	0.253985
	1.021672	0.749739	0.193574	0.555383	2.184444	0.679511	1.268833	0.274065	0.263093	0.370905	1.976904	0.40099
	1.096622	0.851477	0.237121	0.594373	2.323749	0.739562	2.344547	0.528866	0.403646	0.413574	3.107043	0.640911
	1.183616	0.969561	0.378387	0.720859	2.822638	0.954619	2.436014	0.550531	0.579146	0.466853	3.530185	0.730741
	1.194738	0.984658	0.407748	0.747148	2.958892	1.013354	2.452116	0.554345	1.822593	0.844339	4.307384	0.895735
	1.437683	1.314429	1.087597	1.355862	3.10136	1.074768	5.031242	1.165253	4.624008	1.694794	4.626688	0.963521
	1.821433	1.835328	1.483341	1.710199	4.321925	1.60092	5.079784	1.176751	5.824116	2.059123	8.052919	1.690887
	1.842374	1.863753	1.67318	1.880175	6.265355	2.438679	14.46646	3.40014	5.915225	2.086782	9.623879	2.024391
max		2.070502		2.289135		2.438679		3.40014		2.086782		2.54352
mean	0.469334		-0.42671		0.608116		0.111788		-0.95868		0.088056	
stdev	0.736707		1.116859		2.319797		4.221789		3.294019		4.710465	
G	2.810482		2.049619		1.051247		0.805379		0.633506		0.539972	
alpha	0.05		0.05		0.05		0.05		0.05		0.05	
size	25		25		25		25		25		25	
sig value	0.001		0.001		0.001		0.001		0.001		0.001	
df	23		23		23		23		23		23	
t-crit	3.484964		3.484964		3.484964		3.484964		3.484964		3.484964	
G-crit	2.821681		2.821681		2.821681		2.821681		2.821681		2.821681	
significant	no		no		no		no		no		no	

6. Linear Regression

Id number	ECV	ECV^1/3	Sex	Antero-posterior frontal		Antero-posterior occipital		Vertical frontal		Vertical occipital		Lateral frontal		Lateral occipital	
41422	104821	34940.33	F	0.091424	0.091424	0.056599	0.056599	0.2224	0.2224	-4.17435	4.174351	-1.83333	1.833333	-0.4321	0.432103
41425	103532	34510.67	F	0.057194	0.057194	0.046092	0.046092	-0.57269	0.57269	-1.21131	1.211314	0.005227	0.005227	0.395046	0.395046
41437	965754	321918	F	0.290764	0.290764	-0.00175	0.001754	0.285095	0.285095	-0.24427	0.244265	-0.40814	0.408143	0.397404	0.397404
41438	85961	28653.67	F	0.450898	0.450898	0.654649	0.654649	1.368735	1.368735	2.24188	2.24188	-0.07998	0.079981	0.182312	0.182312
41462	99606.4	33202.13	F	0.085163	0.085163	-0.40729	0.407292	1.077172	1.077172	1.129212	1.129212	2.699764	2.699764	1.996684	1.996684
41466	84891.8	28297.27	F	0.14519	0.14519	-0.57149	0.571486	0.523348	0.523348	-0.52146	0.521464	-0.74165	0.741649	-0.14415	0.144148
41473	106639	35546.33	F	0.180386	0.180386	0.019666	0.019666	0.253838	0.253838	0.368659	0.368659	0.191414	0.191414	2.194028	2.194028
41482	102418	34139.33	F	-0.01131	0.011311	-0.53861	0.538608	-0.28291	0.282908	-0.83482	0.83482	0.270965	0.270965	0.01872	0.01872
41488	105454	35151.33	F	-0.19767	0.197669	0.178769	0.178769	-1.74694	1.746943	0.147254	0.147254	0.861081	0.861081	-1.87578	1.875779
41497	95755.7	31918.57	F	0.143271	0.143271	-1.10244	1.102445	1.353684	1.353684	-0.85463	0.854634	2.706198	2.706198	0.326946	0.326946
41535	94282	31427.33	F	0.499114	0.499114	0.016991	0.016991	0.977241	0.977241	-0.56718	0.567182	-0.51637	0.516365	0.899764	0.899764
41550	89522.7	29840.9	F	0.82418	0.82418	0.486533	0.486533	0.507328	0.507328	-0.64983	0.649833	-3.21046	3.210463	-4.02159	4.021588
41413	108689	36229.67	M	0.564858	0.564858	-0.48562	0.485622	-0.86384	0.863837	-1.53531	1.535312	-2.51014	2.510143	1.684713	1.684713
41415	102076	34025.33	M	0.172272	0.172272	-1.39427	1.394266	-0.23907	0.239066	-2.42257	2.422567	-0.08008	0.080078	-3.37493	3.374934
41428	103517	34505.67	M	-0.14011	0.140106	-0.75874	0.758741	0.044335	0.044335	-1.67264	1.67264	-0.365	0.365004	4.518775	4.518775
41431	101762	33920.67	M	0.371725	0.371725	0.781156	0.781156	2.925101	2.925101	6.753946	6.753946	-1.91693	1.916935	-5.55252	5.552524
41447	103864	34621.33	M	0.142936	0.142936	0.111461	0.111461	-0.60231	0.602315	2.364995	2.364995	0.02594	0.02594	-1.35682	1.356816
41461	994936	331645.3	M	0.689388	0.689388	-0.56289	0.562888	-0.55996	0.55996	-0.50943	0.509427	-2.97431	2.974313	-0.72414	0.724144
41467	111262	37087.33	M	0.691479	0.691479	-0.51965	0.519652	1.357597	1.357597	-0.28844	0.288438	-2.70731	2.707314	3.873191	3.873191
41470	72392	24130.67	M	0.759119	0.759119	-0.09444	0.094442	0.910411	0.910411	-0.0046	0.004603	-0.8952	0.895196	0.441218	0.441218
41499	97544	32514.67	M	0.549971	0.549971	-0.55902	0.559021	-0.87508	0.875083	0.584078	0.584078	-2.19463	2.194625	0.591265	0.591265
41529	101465	33821.67	M	-0.18413	0.184134	0.19018	0.19018	-1.55266	1.552661	1.093531	1.093531	2.156704	2.156704	-0.13708	0.137077
41537	92666.7	30888.9	M	0.432363	0.432363	-0.16972	0.169715	0.233531	0.233531	1.10964	1.10964	-0.55685	0.556846	0.570149	0.570149
41544	85825.2	28608.4	M	-0.46581	0.465812	0.085386	0.085386	1.906406	1.906406	0.313846	0.313846	0.116051	0.116051	1.37052	1.37052
41549	91862	30620.67	M	-0.27318	0.273177	-0.72504	0.725036	-0.1072	0.107201	0.097914	0.097914	-0.86416	0.864156	-0.81797	0.817973
Correlation factor (M)					0.351965		0.070633		-0.13598		-0.14228		0.463701		-0.1819
Correlation factor (F)					0.040024		-0.32389		-0.29399		-0.23133		-0.19883		-0.17433
Correlation factor (All)					0.182279		-0.10907		-0.18869		-0.17		0.134739		-0.17067
T value (M)					1.247136		0.234851		-0.45521		-0.47673		1.735819		-0.61351
T value (F)					0.126667		-1.08258		-0.97268		-0.75193		-0.64156		-0.55986
T value (All)					0.889073		-0.52624		-0.92148		-0.82735		0.652131		-0.83068
df (M)					11		11		11		11		11		11
df (F)					10		10		10		10		10		10
df (All)					23		23		23		23		23		23
p-value (M)					0.238248		0.818639		0.65781		0.642888		0.110483		0.552012
p-value (F)					0.901715		0.304408		0.353653		0.469421		0.535584		0.587894
p-value (All)					0.383169		0.603758		0.366363		0.416543		0.520781		0.414697

7. Asymmetry: Directional asymmetry, Absolute asymmetry, FA4a, Kurtosis, Skewness

Id number	Sex	Antero-posterior frontal	Absolute	Antero-posterior occipital	Absolute	Vertical frontal	Absolute	Vertical occipital	Absolute	Lateral frontal	Absolute	Lateral occipital	Absolute
41422	F	0.091424	0.091424	0.056599	0.056599	0.2224	0.2224	-4.17435	4.174351	-1.83333	1.833333	-0.4321	0.432103
41425	F	0.057194	0.057194	0.046092	0.046092	-0.57269	0.57269	-1.21131	1.211314	0.005227	0.005227	0.395046	0.395046
41437	F	0.290764	0.290764	-0.00175	0.001754	0.285095	0.285095	-0.24427	0.244265	-0.40814	0.408143	0.397404	0.397404
41438	F	0.450898	0.450898	0.654649	0.654649	1.368735	1.368735	2.24188	2.24188	-0.07998	0.079981	0.182312	0.182312
41462	F	0.085163	0.085163	-0.40729	0.407292	1.077172	1.077172	1.129212	1.129212	2.699764	2.699764	1.996684	1.996684
41466	F	0.14519	0.14519	-0.57149	0.571486	0.523348	0.523348	-0.52146	0.521464	-0.74165	0.741649	-0.14415	0.144148
41473	F	0.180386	0.180386	0.019666	0.019666	0.253838	0.253838	0.368659	0.368659	0.191414	0.191414	2.194028	2.194028
41482	F	-0.01131	0.011311	-0.53861	0.538608	-0.28291	0.282908	-0.83482	0.83482	0.270965	0.270965	0.01872	0.01872
41488	F	-0.19767	0.197669	0.178769	0.178769	-1.74694	1.746943	0.147254	0.147254	0.861081	0.861081	-1.87578	1.875779
41497	F	0.143271	0.143271	-1.10244	1.102445	1.353684	1.353684	-0.85463	0.854634	2.706198	2.706198	0.326946	0.326946
41535	F	0.499114	0.499114	0.016991	0.016991	0.977241	0.977241	-0.56718	0.567182	-0.51637	0.516365	0.899764	0.899764
41550	F	0.82418	0.82418	0.486533	0.486533	0.507328	0.507328	-0.64983	0.649833	-3.21046	3.210463	-4.02159	4.021588
41413	M	0.564858	0.564858	-0.48562	0.485622	-0.86384	0.863837	-1.53531	1.535312	-2.51014	2.510143	1.684713	1.684713
41415	M	0.172272	0.172272	-1.39427	1.394266	-0.23907	0.239066	-2.42257	2.422567	-0.08008	0.080078	-3.37493	3.374934
41428	M	-0.14011	0.140106	-0.75874	0.758741	0.044335	0.044335	-1.67264	1.67264	-0.365	0.365004	4.518775	4.518775
41431	M	0.371725	0.371725	0.781156	0.781156	2.925101	2.925101	6.753946	6.753946	-1.91693	1.916935	-5.55252	5.552524
41447	M	0.142936	0.142936	0.111461	0.111461	-0.60231	0.602315	2.364995	2.364995	0.02594	0.02594	-1.35682	1.356816
41461	M	0.689388	0.689388	-0.56289	0.562888	-0.55996	0.55996	-0.50943	0.509427	-2.97431	2.974313	-0.72414	0.724144
41467	M	0.691479	0.691479	-0.51965	0.519652	1.357597	1.357597	-0.28844	0.288438	-2.70731	2.707314	3.873191	3.873191
41470	M	0.759119	0.759119	-0.09444	0.094442	0.910411	0.910411	-0.0046	0.004603	-0.8952	0.895196	0.441218	0.441218
41499	M	0.549971	0.549971	-0.55902	0.559021	-0.87508	0.875083	0.584078	0.584078	-2.19463	2.194625	0.591265	0.591265
41529	M	-0.18413	0.184134	0.19018	0.19018	-1.55266	1.552661	1.093531	1.093531	2.156704	2.156704	-0.13708	0.137077
41537	M	0.432363	0.432363	-0.16972	0.169715	0.233531	0.233531	1.10964	1.10964	-0.55685	0.556846	0.570149	0.570149
41544	M	-0.46581	0.465812	0.085386	0.085386	1.906406	1.906406	0.313846	0.313846	0.116051	0.116051	1.37052	1.37052
41549	M	-0.27318	0.273177	-0.72504	0.725036	-0.1072	0.107201	0.097914	0.097914	-0.86416	0.864156	-0.81797	0.817973

				DA = (R -L)		FA1 = |R-L|		FA4a = 0.798(var(R-L))^1/2	Kurtosis	Kurtosis p-value	Skewness
Trait		Sex	N	Mean	SE	Mean	SE				
Frontal	AP	M	13	0.25	0.11	0.42	0.07	0.07	-1.21	ns	-0.44
		F	12	0.21	0.08	0.25	0.06	0.03	0.23	ns	0.97
		All	25	0.23	0.07	0.34	0.05	0.05	-0.08	ns	-0.07
	VERT	M	13	0.20	0.26	0.94	0.15	0.63	-0.44	ns	0.90
		F	12	0.33	0.35	0.76	0.23	0.32	-0.61	ns	-1.09
		All	25	0.26	0.22	0.85	0.14	0.46	-0.28	ns	0.34
	LAT	M	13	-0.98	0.48	1.34	0.34	0.83	0.31	ns	0.49
		F	12	0.00	0.40	1.13	0.30	1.09	0.78	ns	0.02
		All	25	-0.51	0.32	1.24	0.22	1.02	0.93	ns	0.30
Occipital	AP	M	13	-0.32	0.14	0.50	0.10	0.12	0.51	ns	0.09
		F	12	-0.10	0.15	0.34	0.10	0.09	0.13	ns	-0.56
		All	25	-0.21	0.10	0.42	0.07	0.11	-0.94	ns	-0.22
	VERT	M	13	0.45	0.44	1.44	0.32	2.09	-1.48	*	1.77
		F	12	-0.43	0.63	1.08	0.50	0.93	-1.50	*	-0.90
		All	25	0.03	0.39	1.27	0.30	1.55	-1.53	*	1.36
	LAT	M	13	0.08	0.48	1.92	0.35	2.87	-1.40	*	-0.39
		F	12	-0.01	0.74	1.07	0.49	1.09	-1.54	*	-1.26
		All	25	0.04	0.44	1.52	0.31	1.93	-1.45	*	-0.52

Kurtosis values from Palmer and Strobeck 2003 - table 5, values for equation 7)

	Platykurtosis		Leptokurtosis	
	5%	1%	5%	1%
n=12	-1.442	-1.72	2.416	4.248
n=15	-1.284	-1.563	2.152	3.973
n=25	-1.052	-1.288	1.735	3.196

Supplementary Material 2: Calculations

Endocranial shape asymmetries in *Hylobates lar*

Soumik Saha

The three cranial landmarks are the three following position vectors:
Glabella, **g** $\langle g_x, g_y, g_z \rangle$; Inion, **i** $\langle i_x, i_y, i_z \rangle$; Basion, **b** $\langle b_x, b_y, b_z \rangle$.

Let L_1 be the line formed by joining **g** to **i**.
Let $\mathbf{d_1}$ be the directional vector of L_1.

$$\mathbf{d_1} = \mathbf{i} - \mathbf{g} = \langle i_x - g_x , i_y - g_y , i_z - g_z \rangle$$

Then L_1 is given by

$\mathbf{r} = \mathbf{g} + t\mathbf{d_1}$, where t is a scalar factor.

Let **p** be a position vector $\langle p_x, p_y, p_z \rangle$. To project **p** onto L_1, the directional vector that connects **p** to L_1 must be orthogonal to $\mathbf{d_1}$. Orthogonal vectors have a dot product of 0.

Therefore,

$$[\mathbf{p} - (\mathbf{g} + t\mathbf{d_1})] . \mathbf{d_1} = 0$$
$$(\mathbf{p} - \mathbf{g} - t\mathbf{d_1}) . \mathbf{d_1} = 0$$
$$[(\mathbf{p} - \mathbf{g}) . \mathbf{d_1}] - t (\mathbf{d_1} . \mathbf{d_1}) = 0$$
$$t = [(\mathbf{p} - \mathbf{g}) . \mathbf{d_1}] / (\mathbf{d_1} . \mathbf{d_1})$$

Then, to find the position vector of the projection of **p** onto L_1,

$$\mathbf{r} = \mathbf{g} + t\mathbf{d_1}$$
$$\mathbf{r} = \mathbf{g} + \{[(\mathbf{p} - \mathbf{g}) . \mathbf{d_1}] / (\mathbf{d_1} . \mathbf{d_1})\} \times \mathbf{d_1}$$

The above technique was used to calculate the orthogonal projection of the right frontal point (RFP), left frontal point (LFP), right occipital point (ROP), and left occipital point (LOP) onto L_1.

Then, the distance between **g** and the projection of RFP was subtracted from the distance between **g** and the projection of LFP to get the <u>antero-posterior frontal component of petalia</u>.

Similarly, the distance between **g** and the projection of LFP was subtracted from the distance between **g** and the projection of RFP to get the <u>antero-posterior occipital component of petalia</u>. This ensures that a positive value of the petalia component means that the right side is larger than the left.

Next, let the position vector of the the projection of **b** onto L_1 be **w** $\langle w_x, w_y, w_z \rangle$.
Let L_2 be the line formed by joining **b** to **w**.
Let $\mathbf{d_2}$ be the directional vector of L_2.

$$\mathbf{d_2} = \mathbf{w} - \mathbf{b} = \langle w_x - b_x , w_y - b_y , w_z - b_z \rangle$$

Therefore,

$$(\mathbf{b} - (\mathbf{g} + t\mathbf{d_1})) . \mathbf{d_1} = 0$$
$$t = [(\mathbf{b} - \mathbf{g}) . \mathbf{d_1}] / (\mathbf{d_1} . \mathbf{d_1})$$

As per the above calculations, the position vector **w** is

$$\mathbf{r} = \mathbf{g} + \{[(\mathbf{b} - \mathbf{g}) . \mathbf{d_1}] / (\mathbf{d_1} . \mathbf{d_1})\} \times \mathbf{d_1}$$

Then, to project position vector **p** $\langle p_x, p_y, p_z \rangle$ onto L_2, the directional vector that connects **p** to L_2 must be orthogonal to $\mathbf{d_2}$. Orthogonal vectors have a dot product of 0.

Therefore,

$$[\mathbf{p} - (\mathbf{b} + t\mathbf{d_2})] . \mathbf{d_2} = 0$$
$$(\mathbf{p} - \mathbf{b} - t\mathbf{d_2}) . \mathbf{d_2} = 0$$
$$[(\mathbf{p} - \mathbf{b}) . \mathbf{d_2}] - t (\mathbf{d_2} . \mathbf{d_2}) = 0$$
$$t = [(\mathbf{p} - \mathbf{b}) . \mathbf{d_2}] / (\mathbf{d_2} . \mathbf{d_2})$$

Then, to find the position vector of the projection of **p** onto L_1,

$$\mathbf{r} = \mathbf{b} + t\mathbf{d_2}$$
$$\mathbf{r} = \mathbf{b} + \{[(\mathbf{p} - \mathbf{b}) . \mathbf{d_2}] / (\mathbf{d_2} . \mathbf{d_2})\} \times \mathbf{d_2}$$

The above technique was used to calculate the orthogonal projection of the right frontal point (RFP), left frontal point (LFP), right occipital point (ROP), and left occipital point (LOP) onto L_2.

Then, the distance between **b** and the projection of RFP was subtracted from the distance between **b** and the projection of LFP to get the vertical frontal component of petalia.

Similarly, the distance between **b** and the projection of RFP was subtracted from the distance between **g** and the projection of LFP to get the vertical occipital component of petalia.

Finally, let the plain formed by L_1 and L_2 be defined by its normal vector **n** $\langle n_x, n_y, n_z \rangle$.

Recall, the three cranial landmarks are the three following position vectors:
Glabella, **g** $\langle g_x, g_y, g_z \rangle$; Inion, **i** $\langle i_x, i_y, i_z \rangle$; Basion, **b** $\langle b_x, b_y, b_z \rangle$.

$\mathbf{i} - \mathbf{g} = \langle i_x - g_x , i_y - g_y , i_z - g_z \rangle$

$\mathbf{b} - \mathbf{i} = \langle b_x - i_x , b_y - i_y , b_z - i_z \rangle$

The normal of the plane is the cross product of the above two vectors.

So

$$\mathbf{n} = \begin{vmatrix} i & j & k \\ i_x - g_x & i_y - g_y & i_z - g_z \\ b_x - i_x & b_y - i_y & b_z - i_z \end{vmatrix}$$

$$\mathbf{n} = \begin{vmatrix} i_y - g_y & i_z - g_z \\ b_y - i_y & b_z - i_z \end{vmatrix} i + \begin{vmatrix} i_x - g_x & i_z - g_z \\ b_x - i_x & b_z - i_z \end{vmatrix} j + \begin{vmatrix} i_x - g_x & i_y - g_y \\ b_x - i_x & b_y - i_y \end{vmatrix} k$$

$$\mathbf{n} = [(i_y - g_y)(b_z - i_z) - (i_z - g_z)(b_y - i_y)]\, i + [(i_x - g_x)(b_z - i_z) - (i_z - g_z)(b_x - i_x)]\, j + [(i_x - g_x)(b_y - i_y) - (i_y - g_y)(b_x - i_x)]\, k$$

$$\mathbf{n} = [g_y (i_z - b_z) + i_y (-g_z + b_z) + b_y (g_z - i_z)]\, i + [g_z (i_x - b_x) + i_z (- g_x - b_x) + b_z (g_x - i_x)]\, j + [g_x (i_y - b_y) + i_x (g_y - b_y) + b_x (g_y - i_y)]\, k$$

Therefore,

$n_x = g_y (i_z - b_z) + i_y (-g_z + b_z) + b_y (g_z - i_z)$
$n_y = g_z (i_x - b_x) + i_z (- g_x - b_x) + b_z (g_x - i_x)$
$n_z = g_x (i_y - b_y) + i_x (g_y - b_y) + b_x (g_y - i_y)$

Next, let the orthogonal distance from the position vector **p** $\langle p_x, p_y, p_z \rangle$ to the plain defined by normal vector **n** be d.

We are using the position vector **g** $\langle g_x, g_y, g_z \rangle$ as a reference point on the plane.

Let the unit normal vector of the plane be $\mathbf{n_u}$.

$\mathbf{n_u} = \langle n_x, n_y, n_z \rangle / \sqrt{(n_x^2 + n_y^2 + n_z^2)}$

$\mathbf{p} - \mathbf{g} = \langle p_x - g_x , p_y - g_y , p_z - g_z \rangle$

$$d = | (\mathbf{p} - \mathbf{g}) \, . \, \mathbf{n_u} |$$

$$d = \frac{| \langle p_x - g_x , p_y - g_y , p_z - g_z \rangle \, . \, \langle n_x, n_y, n_z \rangle |}{\sqrt{(n_x^2 + n_y^2 + n_z^2)}}$$

$$d = \frac{| n_x (p_x - g_x) + n_y (p_y - g_y) + n_z (p_z - g_z) |}{\sqrt{(n_x^2 + n_y^2 + n_z^2)}}$$

The above formula was used to calculate the orthogonal distance from the right frontal point (RFP) to the plane, the left frontal point (LFP) to the plane, the right occipital point (ROP) to the plane, and the left occipital point (LOP) to the plane.

Then, the orthogonal distance from the left frontal point (LFP) to the plane was subtracted from the orthogonal distance from the right frontal point (RFP) to the plane to get the lateral frontal component of petalia.

Similarly, the orthogonal distance from the left occipital point (LOP) to the plane was subtracted from the orthogonal distance from the right occipital point (ROP) to the plane to get the lateral occipital component of petalia.